

# Lower BW and its impact on the patterning performance

Paolo Alagna<sup>a</sup>, Greg Rechtsteiner<sup>b</sup>, Vadim Timoshkov<sup>c</sup>, Patrick Wong<sup>d</sup>  
Will Conley<sup>b</sup>, Jan Baselmans<sup>c</sup>

a) Cymer LLC, Kapeldreef 75, 3001 Leuven, Belgium

b) Cymer LLC, 17075 Thornmint Court, San Diego, CA 92127

c) ASML Netherlands B. V. De Run 6501, 5504 DR Veldhoven, The Netherlands

d) imec, Kapeldreef 75, 3001 Leuven, Belgium

## ABSTRACT

Patterning solutions based on ArF immersion lithography are the fundamental enablers of device scaling. In order to meet the challenges of industry technology roadmaps, tool makers in the DUV lithography area are continuously investigating all of the interactions between equipment parameters and patterning in order to identify potential margins of improvement. Cymer, a light source manufacturer, is fully involved and is playing a crucial role in these investigations. As demonstrated by recent studies<sup>[1]</sup>, a significant improvement to multiple patterning solutions can be achieved by leveraging light source capabilities. In particular, bandwidth is a key knob that can be leveraged to improve patterning. While previous publications<sup>[1,2]</sup> assessed contrast loss induced by increased bandwidth, this work will expand the research in the opposite direction and will investigate how patterning can be affected by improved image contrast achieved through a reduction in bandwidth. The impact of lower bandwidth is assessed using experimental and simulation studies and provide persuasive results which suggest continued studies in this area.

Keywords : Laser bandwidth, focus blur, chromatic aberration, low bandwidth

## 1. INTRODUCTION

With the delay in the implementation of EUV scanners in high volume manufacturing (HVM), the usage of the DUV immersion lithography continues to enable future lithographic nodes. Industry roadmaps show a tight combination of DUV lithography and Etch due to the use of Litho-Etch<sup>(n)</sup> patterning or by Self-Aligned multiple Patterning solutions. For example, IMEC, Interuniversity MicroElectronics Center (a research institution, in Leuven, Belgium) has presented an interesting forecast of the logic scaling landscape (figure 1) identifying<sup>[3]</sup> DUV-based SADP (Self Aligned Double Patterning) and SAQP (Self Aligned Quadruple Patterning) as crucial methods to achieve the required patterning shrinkage.

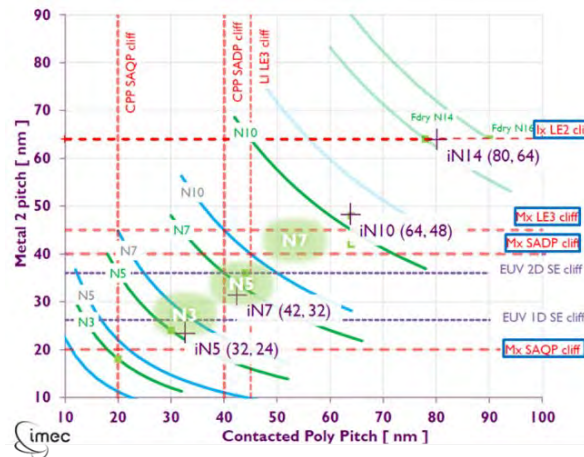


Figure 1. IMEC prevision on the logic scaling landscape

In addition, the ITRS (International Technology Roadmap for Semiconductors) is widely considered a good reference providing estimations and guidelines<sup>[4]</sup> on lithography manufacturing solutions and expected

specifications. Figure 2 shows a summary extracted from latest revision of the ITRS Technology Requirement table.

ITRS Lithography Technology Requirements												
Year of Production	2015	2016	2017	2018	2019	2020	2021	2022	2023	2024	2025	2026
<b>DRAM</b>												
DRAM minimum ½ pitch (nm)	24	22		18.0		15.0			12.0			9.2
CD control (3 sigma) (nm) [B]	2.4	2.2		1.8		1.5			1.2			0.9
Overlay (3 sigma) (nm) [A]	4.8	4.4		3.6		3.0			2.4			1.8
<b>Flash</b>												
2D Flash ½ pitch (nm) (un-contacted poly)	15.5	14.2		11.9		11.9			11.9			11.9
Flash 3D Layer half-pitch targetts (nm)	80.0	80.0		80.0		80.0			80.0			80.0
3D NAND minimum metal pitch(nm)	20.0	20.0		20.0		20.0			20.0			20.0
CD control (3 sigma) (nm) [B]	1.6	1.4		1.2		1.2			1.2			1.2
Overlay (3 sigma) (nm) [A]	5.1	4.7		3.9		3.9			3.9			3.9
<b>MPU / Logic</b>												
MPU/ASIC Minimum Metal ½ pitch (nm)	26	18		12		10			6.0			6.0
MPU/ASIC finFET fin minimum 1/2 pitch (nm)	21	18		12								
Gate CD control (3 sigma) (nm) [B] (10% of gate length)	2.4	1.8		1.4		1.0			1.0			1.0
Metal CD control (3 sigma) (nm) [B] (10% of half pitch)	2.6	1.8		1.2		1.0			0.6			0.6
Fin CD control (3 sigma) (nm) [B] (5% of fin width)	0.40	0.30		0.30								
FIN LER [C]	0.40	0.30		0.30								
Gate LER [C]	2.4	1.8		1.4		1.0			1.0			1.0
Metal LWR [C]	3.9	2.7		1.8		1.5			0.9			0.9
Overlay (3 sigma) (nm) [A]	5.2	3.6		2.4		2.0			1.2			1.2

Figure 2. ITRS Lithography Technology Requirements

Recently, presentations at the SPIE Advanced Lithography conferences have been characterized by a message repeated in almost all sessions which represents the challenges that DUV lithography has to confront: “...every nanometer counts...”. This consistent position clearly shows the market expectations for process and equipment performances improvements: everyone is looking for innovative and creative ways to achieve demanding targets.

If we look more carefully at the table in figure 2, we might realize that the magnitude of changes of the budgets are suggesting that even fractions of nanometers count. Therefore, we might adjust this message by saying that: “...every Angstrom counts...”.

In response to these industry challenges, Cymer has intensively investigated the interaction between patterning and the DUV light source optical<sup>[1,2]</sup> and beam<sup>[5,6,7]</sup> parameters to demonstrate potential areas of improvement.

For example, we previously presented<sup>[1]</sup> an assessment of the E95 bandwidth control range required to obtain optimal patterning performances on 10 nm process node (N10) Metal 1 logic layers (in a LELELE patterning flow). The work presented this year is a significant extension to this previous work and studies the effect of image contrast enhancement achieved through lower E95 bandwidth.

## 2. WHY BANDWIDTH?

Excimer laser bandwidth, specifically E95, can be seen as a finite oscillation (at decreased intensity) of the central wavelength (figure 3). From basic optical theory, there is a tight correlation between wavelength change and lens aberration response<sup>[8,9]</sup>. In an ideal scenario such variation must be kept as closer to zero as possible. In practice, lenses used in the fabrication of the ArF immersion tools are highly chromatic, meaning that small wavelength shifts can cause large focus variation mainly due to Chromatic Aberration (defined as the longitudinal variation of focus, or image position, with wavelength). Noting that the image formation is the result of the superposition of the image intensities of each of the contributing wavelengths, it can be understood why, in a finite bandwidth domain, the image superposition leads to a focus blur. The amount of this blur is directly proportional to the range of wavelengths sampled.

Therefore, the laser bandwidth has a wide influence on many of the lithography key performance indicators: process window, CD Uniformity, MEEF, OPC validity, etc.

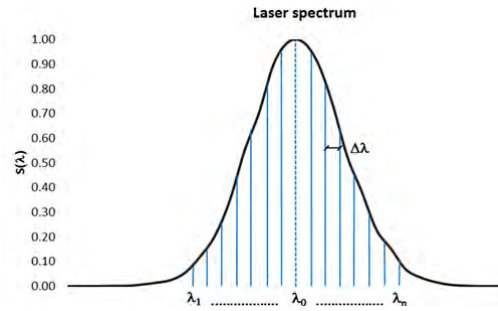


Figure 3. Schematic of finite laser bandwidth

A reduction in E95 bandwidth directly brings a reduction of the imaging blur enhancing contrast as direct consequence.

The target of this work is to explore the patterning performances changes at lower bandwidth in a 300nm optimized OPC regime, and assess the potential margin of improvement **through simulations**. The nominal E95 value for the laser is 300 nm, and in these experiments a lower bandwidth value of 200 nm was targeted and met with an average of 200 nm and  $3\sigma$  of 7.8nm (measurement performed over more than 10K consecutive exposure fields, see figure 5).

### 3. EXPERIMENTAL DATA

The experimental activities in this study have been carried out in IMEC's research facilities in Leuven (Belgium) where a Cymer light source model XLR<sup>®</sup> 760ix supplied laser light to an ASML NXT: 1970Ci scanner. Leveraging previous well-developed processes and a solid metrology, the effects of lower bandwidth on the patterning KPIs for three different type of features (SRAM, Logic, and Line-Trench) were studied.

MEASURED BANDWIDTH E95 (nm)	SRAM	HOT SPOTS	LINE-SPACE	N10 M1 stack
<p>Bandwidth E95 experimentally measured 25 consecutive wafers, 429 exposure fields each wafer</p> <p>Average= 200nm <math>3\sigma = 7.8</math> nm 10725 consecutive exposure fields</p>				
Sampling	<b>4 Features</b> 4 IntraField 10 + 10 Wafers	<b>5 Hot spots</b> 4 IntraField 5 + 5 Wafers	<b>13 CD/Pitches</b> Up to 104 Intrafield 5 + 5 Wafers	<b>Freeform source</b>
KPI measured	- Process Window	- Process Window - CD Uniformity - Profile	- Process Window - CD Uniformity - Roughness - MEEF - Profile	

Figure 5. Experimental condition summary

It is important to note that the studies reported here were performed on masks with OPC models optimized at 300 nm, and not the 200 nm used during exposure.

#### 3.1 SRAM results

For the SRAM feature, a reduced stack (only SOG and SOC and then resist) was used. A total of 20 wafers (10 for each bandwidth condition) were exposed and a total of 228 measurements per wafer/target (4 point per field x 57 exposure fields) were collected. Four different features, as described in figure 6, were selected.

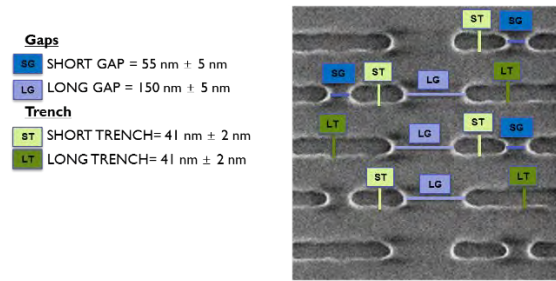


Figure 6. SRAM measurement scheme

The Short Gaps (SG) were targeted at 55 nm ( $\pm$  5 nm), the long gaps (LG) were targeted at 150 nm ( $\pm$  5 nm), and the Short and Long Trenches were targeted at 41 nm ( $\pm$  2 nm). A Hitachi CG-5000 tool was used with the following settings:

*Beam setting: 500V, 8pA*

*Image setting: 200 kX, 16 frames, 512 x 512 window*

The CD measurements were performed using the *Offline CD Measurement Software Off-line Tool* installed on a Hitachi *Terminal PC*.

The comparison of the single and common EL vs. DOF plot is shown in figure 7, highlighting that the process performances at reduced bandwidth are well aligned. A marginal improvement (+0.3%) of the maximum exposure latitude with basically no impact on the maximum DOF was observed.

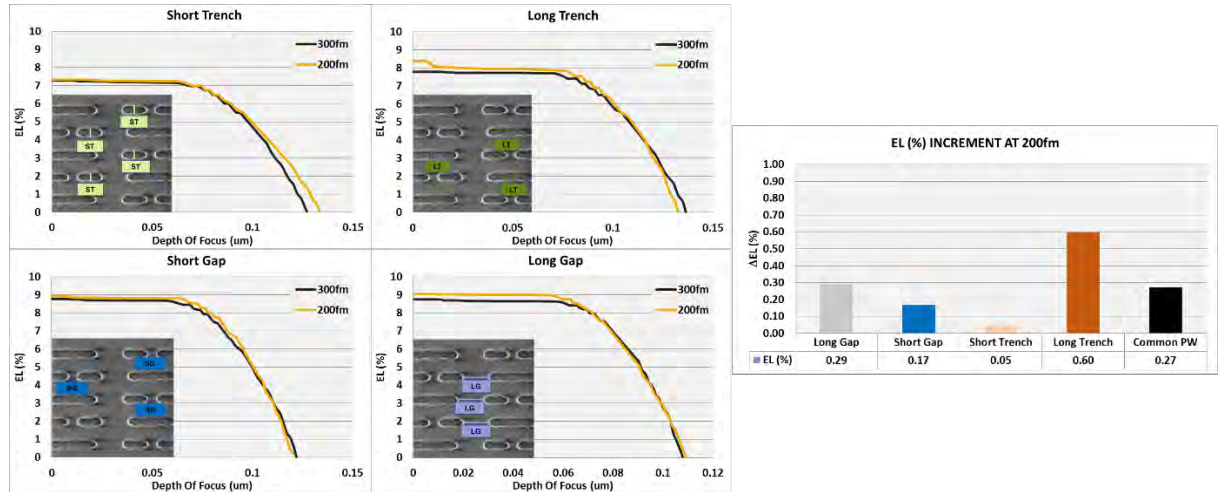


Figure 7. SRAM process windows

### 3.2 N10 Metal 1 Logic features

Similar to previous studies<sup>[1,2]</sup>, the response of the first split of a LELELE process was characterized. Changes in the KPIs as function of bandwidth were analyzed on the five different features reported in figure 8 at after litho (ADI) and after etch (AEI) steps.



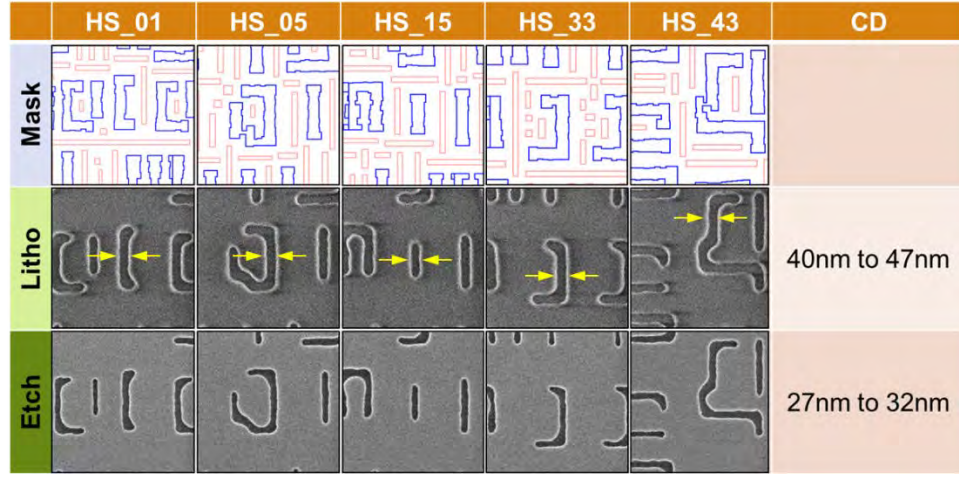


Figure 8. N10 Metal 1 logic feature and CD-SEM measurement point.

Four points per field were measured a CD-SEM Hitachi 5000 with the following settings:

*Beam setting: 500V, 8pA*

*Image setting: 200 kX, 16 frames , 512 x 512 window*

The Process Window analysis was performed on two FEM (Focus Exposure Matrix) wafers at each bandwidth condition (300 fm nominal and 200 fm), with the dose and focus centered at the anchor feature (pitch 96 nm CD 39nm) conditions. Five nanometer focus steps and 0.5 mJ/cm<sup>2</sup> dose steps were used.

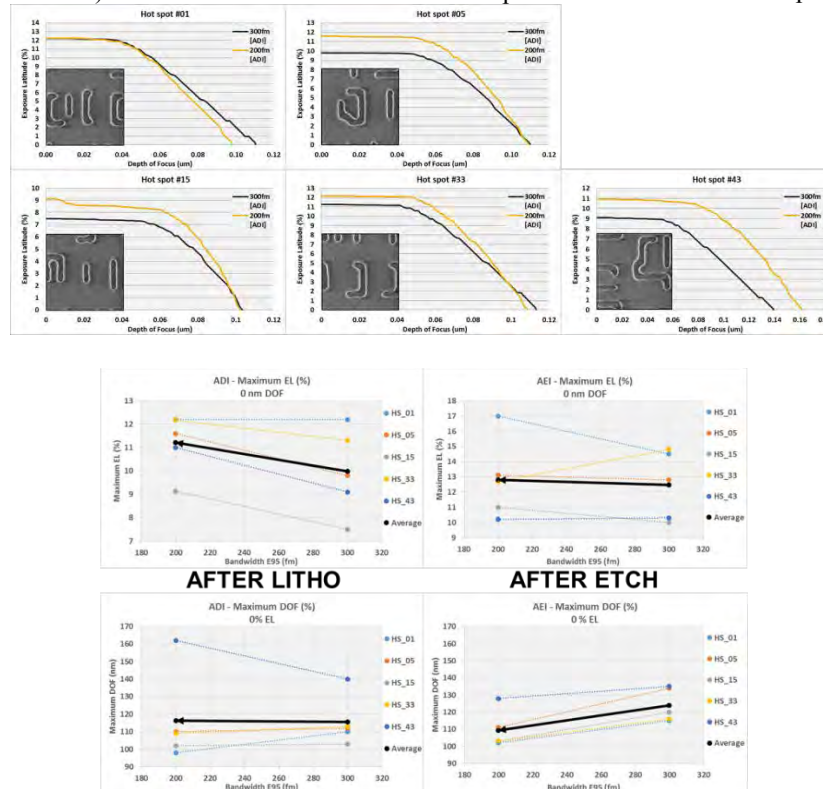


Figure 8. N10 Metal 1 logic features DOF vs. EL plots.

The results reported in figure 8 show an increase in the maximum exposure latitude (EL) induced by the higher imaging contrast of lower E95 bandwidth. The distribution observed across the five hot spots can be explained by a combination of factors such as the intrinsic characteristics of the feature and the optical

proximity being uncorrected for 200 fm. Averaging the EL measurements on all the hot spots, a net improvement of approximately 1% is observed with only a minimal reduction in depth of focus.

There are two important considerations to take into account: 1) the OPC mismatch at 200 fm plays a crucial role in the assessment of the net benefits, and 2) different etch processes might have different responses. Additional work is required to further characterize this response.

CD Uniformity was checked exposing two wafer at each bandwidth condition using the same exposure focus and dose which was used for the anchor feature. Using the local CDU analytical model developed by ASML and IMEC<sup>[10]</sup>, it can be seen from the last term of this equation how the CDU is dependent on the CD and CD sensitivity for a given feature.

### Local CDU analytical model

$$SN[3\sigma, nm] = 3 \sqrt{\frac{1 + F_{AC}}{F_{AC}} \frac{h\nu}{\alpha E_{th}}} \cdot \sqrt{\frac{1}{A} \cdot \frac{dCD}{dD} D}$$

resist parameters     averaging area defined by metrology and  $\sigma_{blur}$      normalized dose sensitivity

This consideration is important because keeping the same dose to size for both samples while changing the contrast (using E95 bandwidth) may have impacted the CD and therefore the CDU measurement. However, the CD data reported in the in figure 9 shows that a contrast-induced CD change may be of the magnitude of less than 1 nm. Therefore, with good approximation, the data calculated can be representative of the effective patterning response.

The sampling scheme includes four intra-field points measured over the central 25 exposure fields (4x5 matrix).

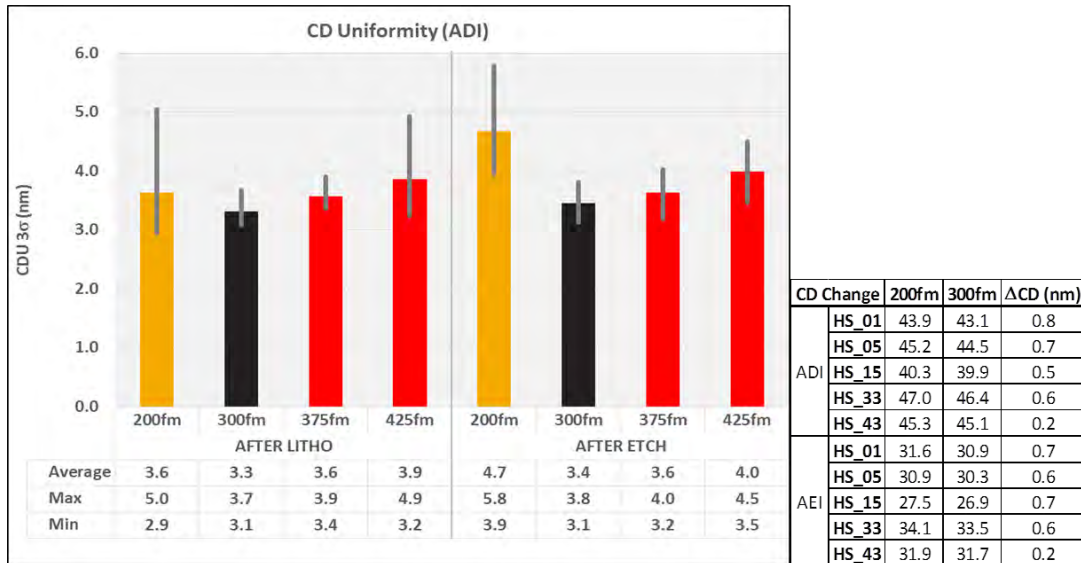


Figure 9. CD change N10 Metal 1 logic features DOF vs. EL plots.

The ADI and AEI data sets in figure 9 show that bandwidth variation modulates CDU. However, looking at the significant spread of the data across the hot spots, it can be reasonably assumed that OPC model optimization at 200 fm may minimize this distribution.

Two approaches were followed to assess how much an increase in contrast affects the profile of the features considered: litho-etch bias (LEB) measurement and AFM inspection. The simulations performed by ASML<sup>[11]</sup> on a generic NTD process, and reported in figure 10, show how changes in side wall angle (SWA), CD and LEB are linked. Looking at the trend shown, it can be concluded that there is almost a linear correlation between changes in SWA and LEB (in absolute value).

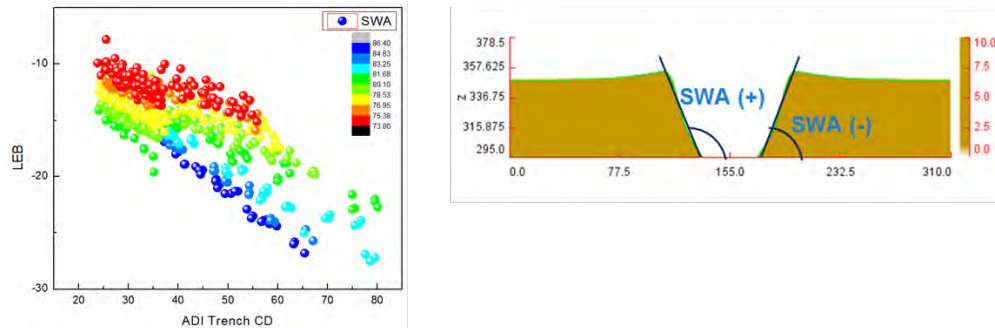


Figure 10. CD changeN10 Metal 1 logic features DOF vs. EL plots.

The simulation results were used as an indicator to interpret the measured data. As showed in figure 9, the difference in bandwidth introduced a marginal shift in effective dose, but given the magnitude of the  $\Delta$ CD values those changes can be considered not significant for the final profile assessment. The conclusion is that the image contrast enhancement has a negligible effect on the profile of the hot spots considered and the Litho-Etch bias value across the features shows comparable results across the 5 hotspots. The well overlapped profiles as measured by AFM confirm this conclusion.

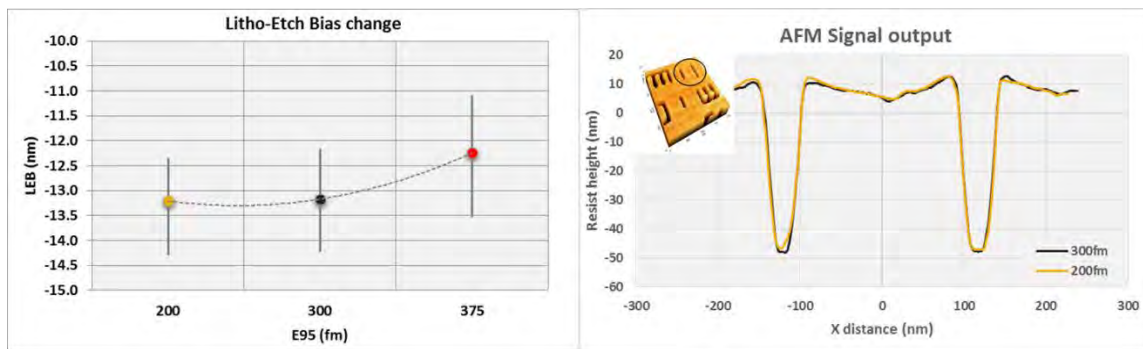


Figure 11. CD changeN10 Metal 1 logic features DOF vs. EL plots.

The profile response was also studied on different pitches of line-trench features on a PTD processes. The measurements were performed on 6 different pitches (92 nm, 104 nm, 128 nm, 160 nm, 200 nm, 280 nm) at 12 intrafield locations using ASML YS-200 scatterometry system. The summary reported in figure 12 shows the SWA measurement change at 200 fm with respect to the nominal conditions, clearly indicating that an E95 reduction has a significant impact on the profile of the most contrast sensitive features.

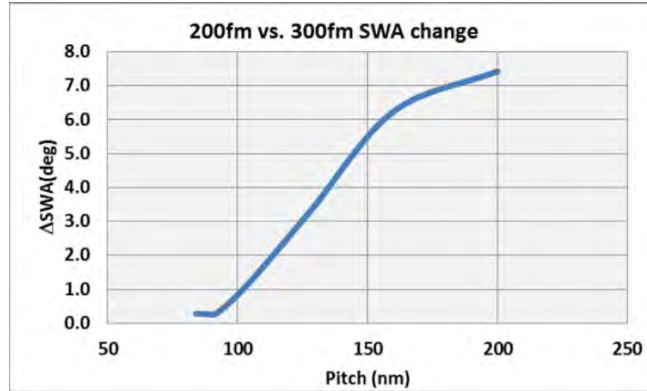


Figure 12. SWA relative change measured on PTD features by YS-200

In addition, the reduction of the imaging blur due to lower E95 bandwidth and the impact on the fidelity of the pattern transferred was studied. The contours after etch on a wafer exposed at 200 fm were extracted and were compared the nominal condition data; 100 measurements per contour were averaged using the sampling scheme used for the CDU sampling..

Using BRION's TFLEX platform, the effective after etch pattern contours to the target were overlaid and the overlap area was calculated. The results obtained show an improvement in pattern coverage area of 1%.

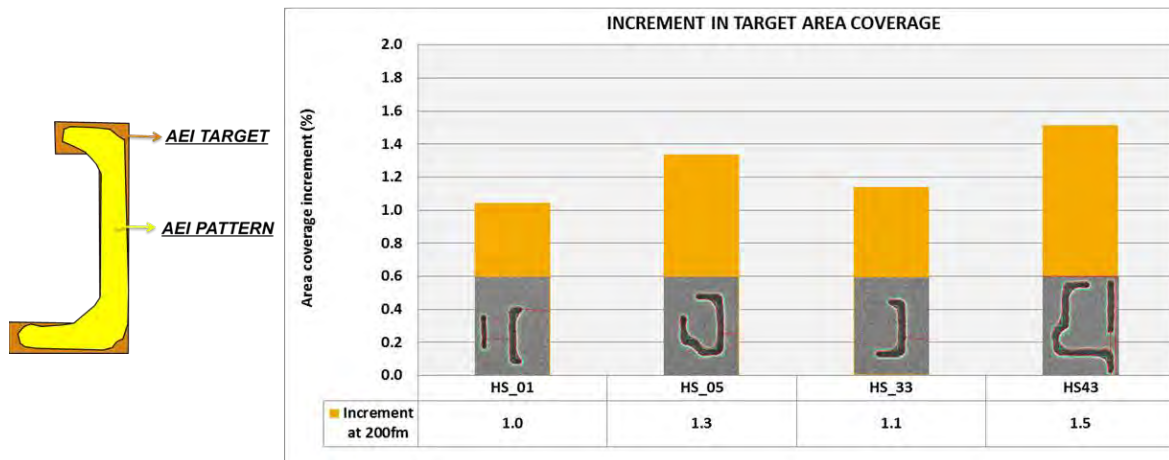


Figure 13. Contour analysis

The primary driver of this increase can be observed in the line-ends which, as already demonstrated<sup>[1]</sup>, are the most bandwidth sensitive part of the patterns.

Measurement of the impact on low bandwidth exposure on roughness (measured at the anchor feature pitch 96 nm CD 39 nm) was assessed using PSD analysis on more than 200 measurements per E95 condition. The settings applied to the CD-SEM Hitachi 5000 during these measurements were:

*Beam setting: 500V, 8pA*

*Image setting: 200 kX, 32 frames, 512 x 512 window*

Figure 14 shows that the response in frequency of pattern roughness does not significantly change with the reduction of the bandwidth from 300 fm to 200 fm. Note that the area below each line is proportional to the CDU ( $\text{IPSD} \sim \text{LCDU}^2$ ). Inspection of this graph shows that increasing imaging blur caused by the exposure performed at 450 fm E95 bandwidth caused roughness degradation at almost all frequencies.



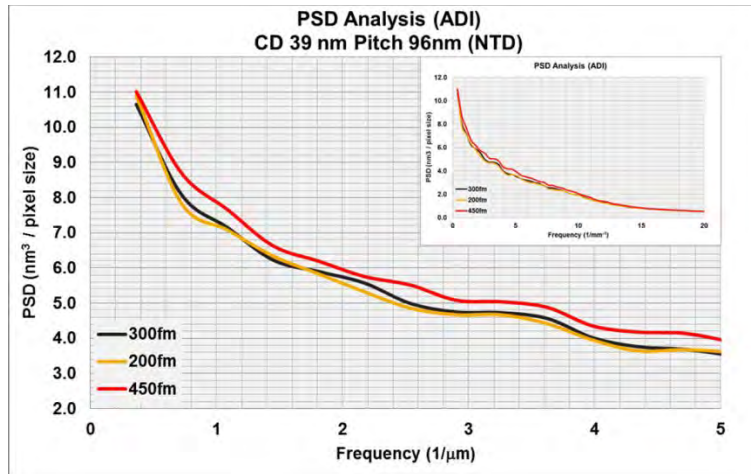


Figure 14. PSD analysis on Pitch 96 CD 39 (linear scales)

In addition, the response of different combinations of line-tranches using a PTD process was studied. using a test mask with a wide selection of CDs and pitches.. A production representative range of features was selected: six different Pitch/CD combinations (nm/nm) including 92/45,104/51,128/62,160/72, 200/84, 280/96.

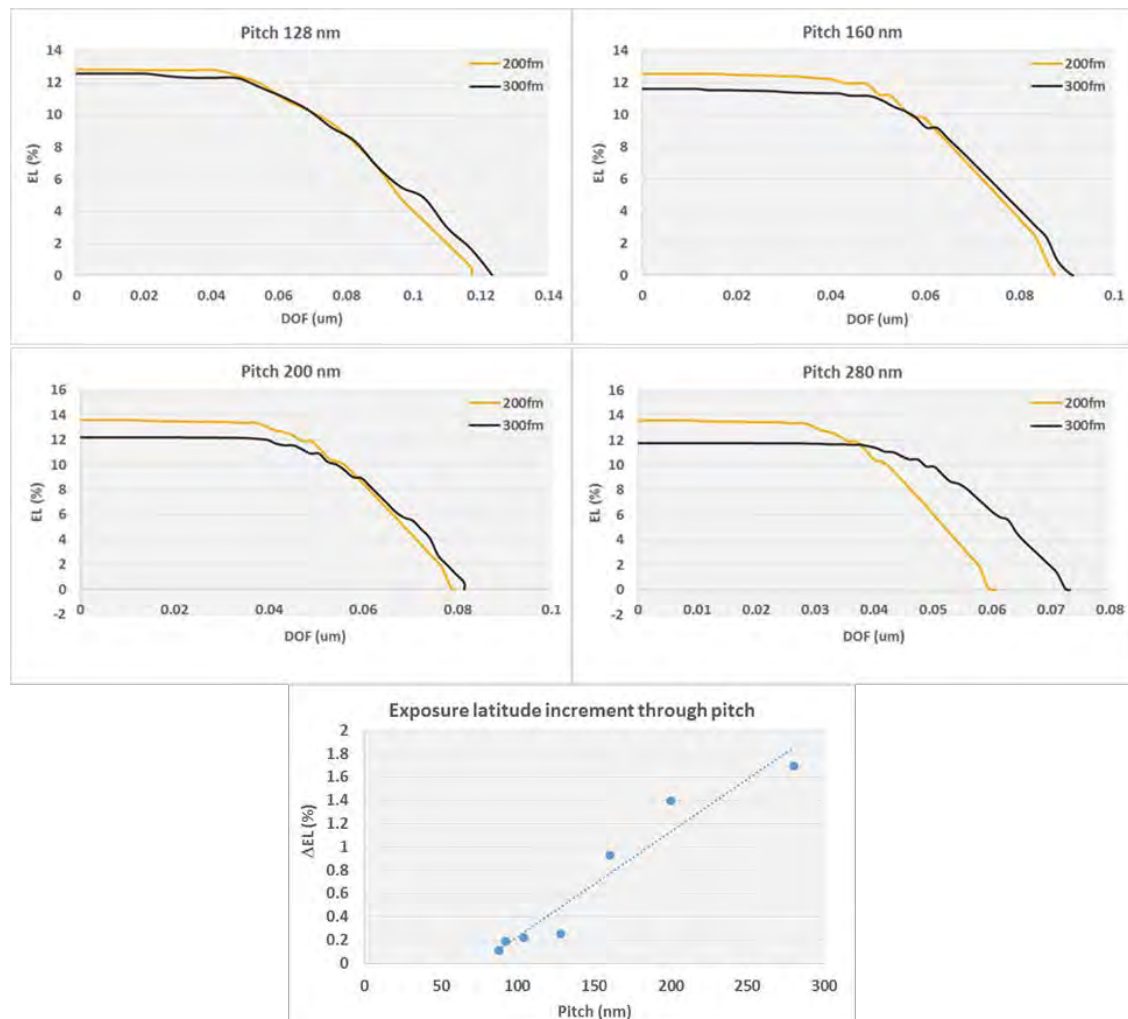


Figure 15. PTD resolved line-tranches, common process window and maximum EL through pitch

As expected we have measured a pitch dependent response, with a general increment of the EL (up to +2%) and a marginal loss in depth of focus (up to -10nm).

**CD Uniformity** performance was assessed using a very high density sampling scheme (104 point per field measured). The tendency showed in figure 16, perhaps due to the less aggressive OPC used on the periodic features, indicates a clear potential for CDU improvement through contrast enhancement.

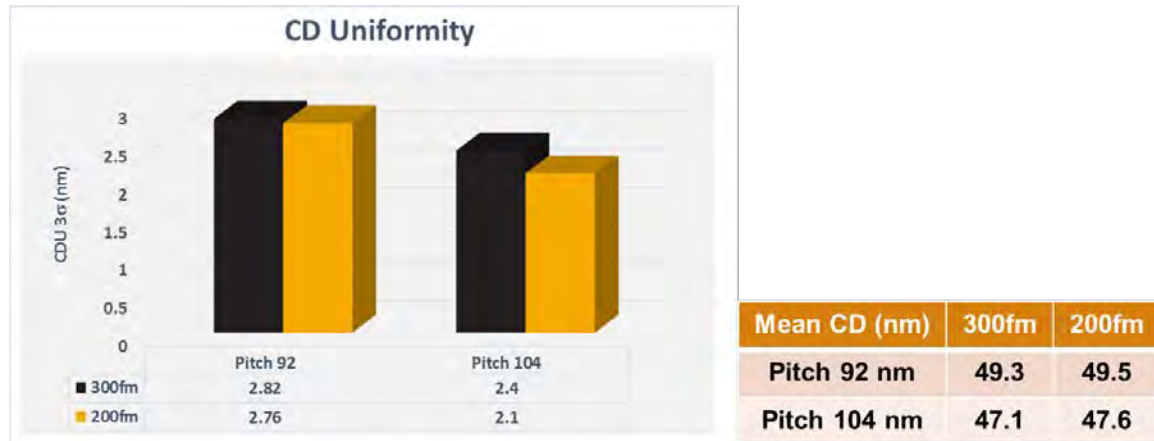


Figure 16. CD uniformity on line-pitch feature resolved on PTD

It may be assumed that a significant contribution to such improvement tendency might come from to the Mask Error Enhancement Factor (MEEF). A reduction in MEEF in the range of 1.8% to 5% (pitch depended) was observed, as shown in figure 17.

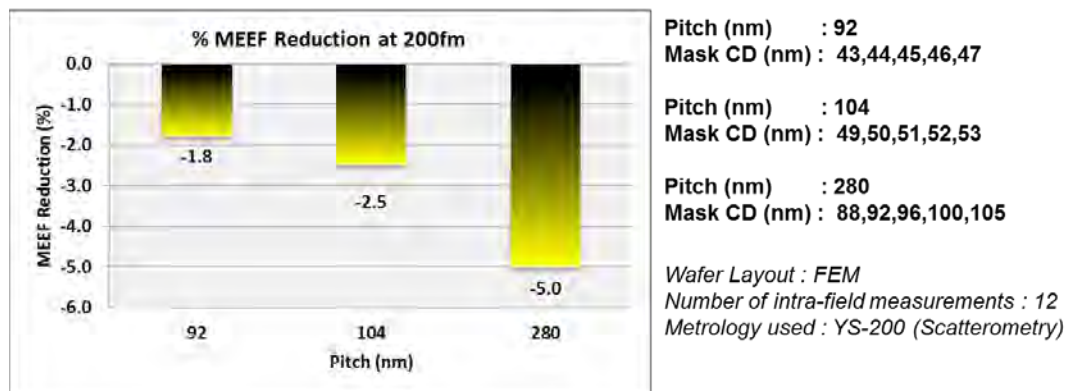


Figure 17. MEEF reduction (%)

#### 4. SIMULATION DATA

NO DATA AVAILABLE. WAITING FOR BRION

#### 5. CONCLUSIONS

The response of patterning key performance indicators to the increases in imaging contrast was studied in detail. Patterns defined in both negative tone development and positive tone developments processes were investigated. In both cases, no OPC corrections to compensate changes in imaging contrast were applied.

In addition, on-wafer verification performance on N10 Metal 1 logic features using mask with 200 nm E95 BW optimized OPC, SMO and OPC simulation studies including customer specific use cases will be the next area of investigation in order to more concretely assess the improvements which can be obtained by the increment in imaging contrast.

The results obtained can be summarized as follows:

PARAMETER	SRAM	LOGIC HS	LINE-TRENCHES
Process Window	EL = +0.3%	EL = +1% (mean) $\Delta$ DOF = -10 nm (mean)	EL up to +1.8% pitch dependent (PTD)
CD Uniformity	-	Degradation due to OPC optimized at different E95	Signs of CDU margins of improvement on regular patterns.
Profile	-	No significant impact	Measures performed on PTD showed pitch related responses.
Pattern fidelity	-	+1% of coverage area	Improvement expected but not measured.
MEEF	-	-	Up to 5% reduction from nominal value (pitch dependent)
Roughness	-	-	No signs of degradation at 200nm

#### ACKNOWLEDGEMENTS

The authors would like to acknowledge Joost Bekaert (imec), Stephen Hsu, David Rio (BRION) Remo Petrella, Aleks Simic, Thomas Ghiese (Cymer) and Julien Mailfert (former at imec) for their assistance on this work, and Maria Kilitziraki and Liesbeth Reijnen for the fruitful technical discussions.

## References

- [1] P. Alagna et al., "Optimum ArFi laser bandwidth for 10nm node logic imaging performance"  
Proc. SPIE 2015, Optical Microlithography XXVIII, 9426,09
- [2] W. Conley et al., "Impact of bandwidth on contrast sensitive structures for low k1 lithography"  
Proc. SPIE 2015, Optical Microlithography XXVIII, 9426,07
- [3] Extracted from the presentation gave by Diederik Verkest (imec) during the October 2015 session of IMEC Program Technical Week.
- [4] Source [www.itrs.net](http://www.itrs.net)
- [5] P. Alagna et al., "Lithography imaging control by enhanced monitoring of light source performance"  
Proc. SPIE 2013, Optical Microlithography 8683,28
- [6] P. Alagna et al., "Improving on-wafer CD correlation analysis using advanced diagnostics and across-wafer light source monitoring"  
Proc. SPIE 2014, Optical Microlithography 9052,28
- [7] P. Alagna et al., "Advanced process characterization using light source performance modulation and monitoring"  
Proc. SPIE 2015, Optical Microlithography 9426,49
- [8] P. De Bisschop et al., " Impact of finite laser bandwidth on the critical dimension of L/S structures",  
J.Micro/Nanolith.MEMS MOEMS 7 (3), 033001 (Jul-Sept 2008)
- [9] T. Brunner et al., "Laser bandwidth and other sources of focus blur in lithography",  
J.Microlith., Microfab.,Microsyst. 5(4), 043003 (Oct-Dec 2006)
- [10] Lorusso et al., "Influence of etch process on contact hole local critical dimension uniformity in extreme-ultraviolet Lithography"  
Proc. SPIE 2014, Advances in Patterning Materials and Processes XXXII 9425,20
- [11] Credits to Roy Anunciado (ASML)



## Technical Publication Board (TPB) – Review page

General remarks only, to be filled in by TPB reviewers.

Detailed remarks are made in the document using track changes.

### Discipline: CIP

Name	Date	Comments
Jeff Brooks	18 Feb 2016	Approved with edits as shown p4 and p12

### Discipline: Technology

Name	Date	Comments

### Discipline: Marketing

Name	Date	Comments

### Discipline: Communications

Name	Date	Comments

### Discipline: Investor Relations

Name	Date	Comments

### Discipline: Manager

Name	Date	Comments

# Neon Reduction Program on Cymer ArF Light Sources

Dinesh Kanawade, Yzzer Roman, Ted Cacouris, Josh Thornes, Kevin OBrien,  
Cymer LLC (an ASML Company),  
17075 Thornmint Ct., San Diego, CA, 92127, USA

## ABSTRACT

In response to significant neon supply constraints, Cymer has responded with a multi-part plan to support its customers. Cymer's primary objective is to ensure that reliable system performance is maintained while minimizing gas consumption. Gas algorithms were optimized to ensure stable performance across all operating conditions.

The Cymer neon support plan contains four elements: 1. Gas reduction program to reduce neon by >50% while maintaining existing performance levels and availability; 2. short-term containment solutions for immediate relief. 3. qualification of additional gas suppliers; and 4. long-term recycling/reclaim opportunity. The Cymer neon reduction program has shown excellent results as demonstrated through the comparison on standard gas use versus the new >50% reduced neon performance for ArF immersion light sources. Testing included stressful conditions such as repetition rate, duty cycle and energy target changes. No performance degradation has been observed over typical gas lives.

**Keywords:** DUV, Neon, GLX, neon recycle, neon reclaim

## 1. INTRODUCTION

Cymer's dual chamber XL light sources [1] have been used for DUV lithography in the semiconductor industry for over a decade, and have a history of continuous improvements in availability [2] and cost reduction over time [3]. Cymer's excimer light sources use Master Oscillator (MO) and Power Ring Amplifier (PRA) chambers that are filled with a mixture of gases under pressure to generate pulsed laser light [4]. The halogen gas used in the laser gain medium is fluorine and the buffer gas is neon, which accounts for the majority of the gas in the MO and PRA chambers. Similarly, in Cymer's single chamber ELS light sources [5] the buffer gas used in the chamber is neon.

Cymer has the industry's largest light source installed base (approximately 2,500 light sources operating across 150+ facilities worldwide) and is committed to reduce the impact of neon availability and the sudden price increases on chipmakers. In response to the neon supply concerns, Cymer initiated and implemented the Neon Reduction Program that reduced the amount of operational gas used, thereby having a direct impact on the neon supply shortage and the running cost for the chipmakers.

### 1.1 Industry demands

Semiconductor applications and processes, specifically lithography, account for the majority of the neon global demand, as neon gas has been used extensively since the introduction of DUV lithography systems in the semiconductor industry. Approximately 70% of the global neon production is used in IC lithography [6]. This demand has been significantly increasing recently, aided by the growing demand in the Asia-Pacific region. The global specialty gas has a forecasted market value of \$23B (USD) by the year 2018 [7].

### 1.2 Industry outlook

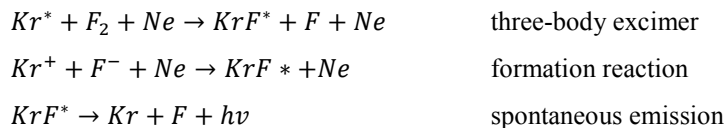
Neon and other rare gases are present in air at very low concentrations (<20ppm) that require intensive processes for its production. Generally, neon is produced through a cryogenic air separation process [8] that requires the construction of air separating units costing upwards of millions of dollars. Cryogenic separation of neon production is generally an addition to rare gas capabilities installed in oxygen plants [6].

Neon gas supply is primarily restricted to Eastern Europe, and specifically to the Ukraine. Recent conflict in this region has further increased supply instability and price volatility, sending Neon prices upwards of 10 times previous rates [9] [10]. This instability generated business continuity concerns in chipmakers.

## 2. BACKGROUND

### 2.1 Why is neon used?

Rare gas halogens such as KrF\* and ArF emit deep ultra-violet photons, 248 and 193nm respectively, when excited by a fast electrical circuit [11]. For optimum discharge and gain conditions a buffer gas that does not react with Krypton or Fluorine is required. Neon gas is an ideal buffer gas that promotes the creation of excited dimers through three-body reactions; for example the KrF reactions are:



Additionally, Neon gas does not absorb wavelengths in the DUV emission regions noted above.

### 2.2 Alternatives to neon

Helium gas was explored as a buffer gas but does not achieve the performance of Neon. Furthermore, it has also recently been subject to supply constraints. Other noble gases have also been explored but are more expensive, unsafe, or do not efficiently promote the generation of excited dimer species.

## 3. NEON USE ASSESSMENT

Neon makes up approximately 96% of the gas content of the bi-mix and tri-mix used in Cymer's excimer light sources. Bi-mix gas primarily contains a composition of Argon and Neon for Argon-Fluoride light sources (typically dual chamber), and Krypton and Neon for Krypton-Fluoride light sources (typically single chamber). Tri-mix gas includes a 1% Fluorine content in addition to the buffer gas. During normal operation, light sources require a periodic gas 'refresh' (through injects or completely through refills) to replenish depleted halogen gas and to remove byproducts of the excimer discharge which decrease system efficiency [12].

On Cymer light sources, GLX™ gas control uses periodic gas injects (bi-mix and tri-mix) to maintain stable performance. The majority of the gas usage under GLX technology is through injects. For systems without GLX technology, refills account for the bulk in gas usage.

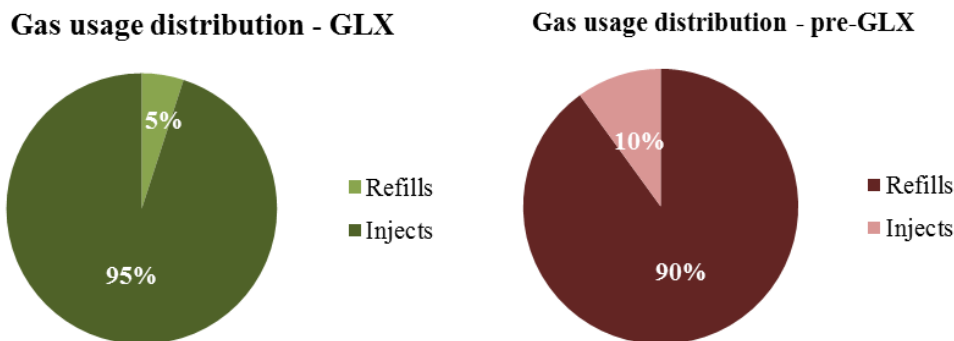


Figure 1- Gas usage distribution for light sources based on gas management technology

### 3.1 Gas consumption calculations

Gas consumption is highly dependent on light source operating conditions. Consumption rates of 5,000L/Bp are typical for ArF systems with GLX technology and yearly utilization of 40Bp/yr. As short term containment action, Cymer provided immediate gas savings by using pre-GLX gas management approaches. Reverting to a pre-GLX gas management reduces both gas consumption and system availability [13]. This containment solution (released in June 2015) provided chipmakers with immediate gas savings of nearly 50%.

The first generation solution for neon reduction (released in September 2015) provided chipmakers with immediate gas savings up to 50% without any light source performance or availability impact. The second generation neon reduction for ArF systems provides up to 75% gas savings by reducing the gas rate use to 1,250L/Bp for systems with a yearly utilization of 40Bp. Figure 2 illustrates the comparison between average usage rates of the released solutions.

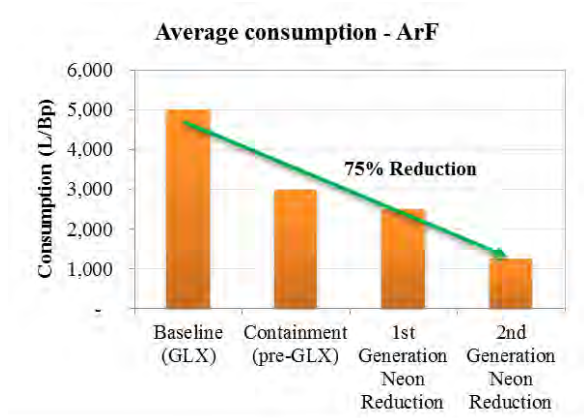


Figure 2- ArF Light source (dual chamber) gas consumption for a system with an average yearly utilization of 40Bp

Similarly, containment solution for KrF (single chamber) systems with GLX technology was to revert to pre-GLX gas management approaches. Reverting to this configuration would provide immediate gas savings of approximately 35%. Further gas savings of up to 30% was achieved by extending the pulse-based interval between refills.

KrF systems that primarily use a legacy gas technology management achieved a ~30% reduction in gas consumption by extending the pulse-based interval between each refill. As indicated earlier, the majority of the gas consumption in these light sources is primarily driven by refills.

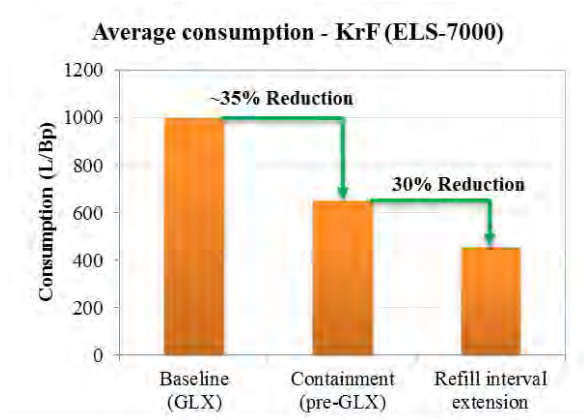


Figure 3 – KrF (ELS-7000) single chamber gas consumption for a system with a yearly utilization of 20Bp

3.2 Cymer gas algorithm developments

As indicated earlier, injects account for the largest portion of neon consumption in Cymer light sources with GLX technology. Therefore, the neon reduction solution targets reduction of these injects. To achieve >50% neon gas reduction, the volume and frequency of injects are reduced. Light source performance remains stable during normal operation after neon reduction without complete gas replenishment until 2Bp. Figure 3 shows E95 bandwidth performance stability during internal tests (200Mp).



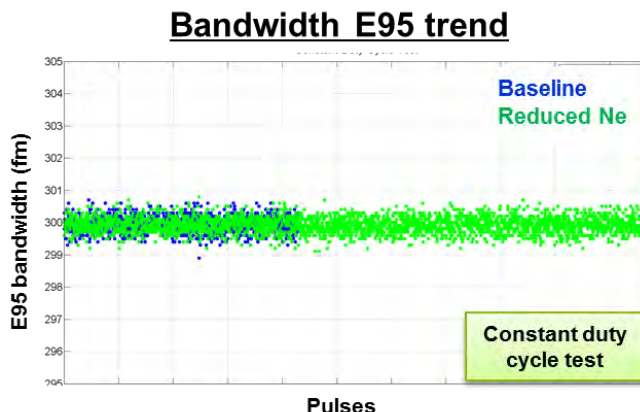


Figure 4- E95 Bandwidth performance for a light source during constant duty cycle with >50% neon reduction

## 4. REDUCTION AND RESULTS

### 4.1 XL systems

Cymer's neon reduction program has resulted in gas savings for ArF Light Source of 150,000 liters at STP per year per light source. Savings are based on the standard GLX rate of 5,000 L/Bp for a light source with 40Bp/yr utilization and the average rate of 1,250 L/Bp for the second generation neon reduction. These gas savings translate to an annual savings of \$450k per system, when based on a neon price of \$3/L.

Cymer's first generation of neon reduction has been installed in over 300 systems worldwide, with a high customer acceptance rate. The second generation of neon reduction has been installed in over 70 tools in the first few weeks after its introduction. Progressive neon savings to date have totaled approximately 2 million liters or \$6 M (USD) across ArF and KrF platforms.

The significant reduction in neon gas consumption has relaxed the supply constraints worldwide and allowed chipmakers to continue normal operation.

## 5. NEON RECAPTURE AND RECYCLING

Cymer continues to support efforts to recapture the used neon gas from light sources for offsite processing by enabling the recapture of the gas. Neon recovery enables effluent process gas to be returned to gas suppliers for purification and reuse. This recovery process creates additional supply of neon within the gas supply chain. The neon collection and compression system along with the gas bottles for storage and transport are to be located within the fab or facilities areas. The gas recycling is to be done at the gas supplier facilities.

Recovery kits have been provided and installed at multiple customers worldwide.

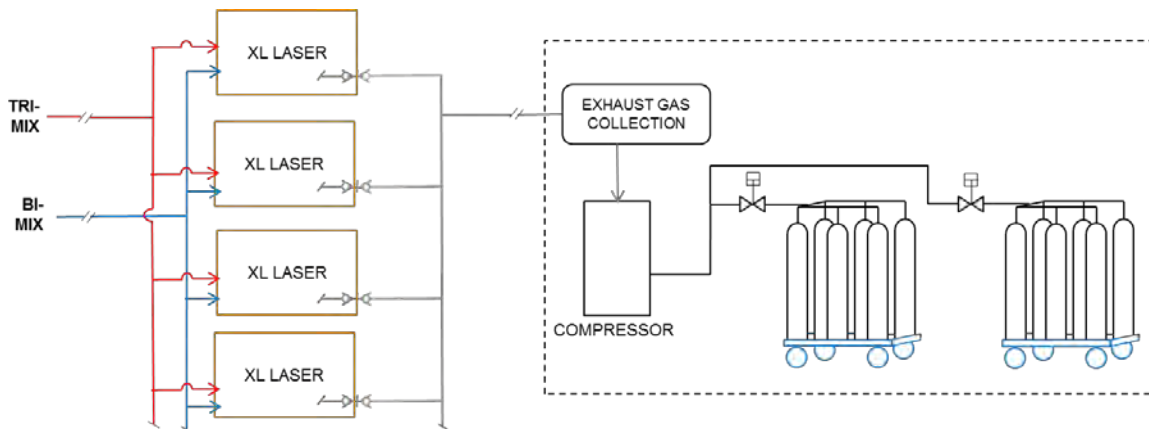


Figure 5 - Neon recovery connection schematic at typical fab

Additionally, Cymer is facilitating gas reuse by developing a unit to provide in-situ recycling through a sequence of filtering and mixture reconstitution. Neon recycling allows for discharged process gas to be reused as bi-max gas to reduce the overall gas consumption for connected light sources. Collected exhaust gas is purified and mixed to the appropriate levels to the bi-mix gas specification. The recycled mixture is introduced to the bi-mix supply distribution.

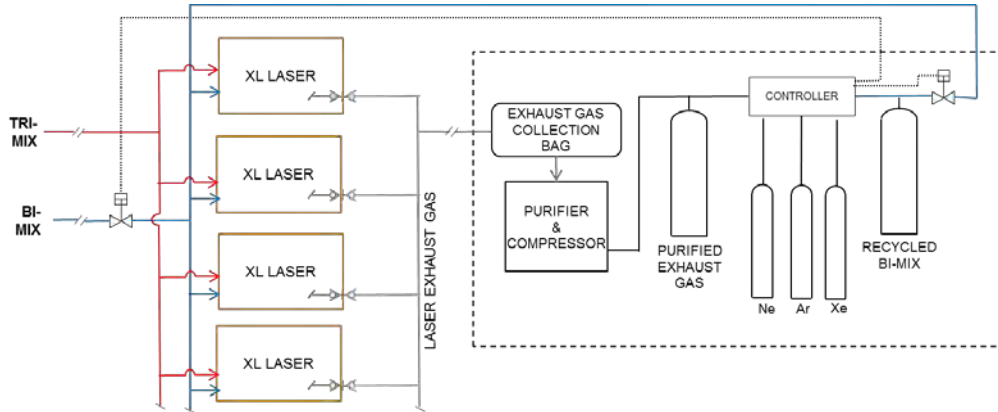


Figure 6- Recycle concept schematic

## 6. CONCLUSIONS

Cymer's neon reduction program provides chipmakers with several avenues to reduce the neon gas consumption. The first generation of the program allowed gas reduction by 50% using proven gas technology. The second generation further reduced consumption up to a total of 75%. Cymer's goal to provide neon reduction solutions without impact to system performance has been achieved. This program has successfully eased supply constraints and resulted in significant neon savings for the semiconductor industry that will amount to over 70 million liters per year, or more than \$200M.

## 7. REFERENCES

- [1] Cymer LLC, "Cymer Products," [Online]. Available: <http://www.cymer.com/duv>. [Accessed 2016].
- [2] K. O'Brien, W. J. Dunstan, D. Riggs, A. Ratnam, R. Jacques, H. Besaucele, D. Brown, K. Zhang and N. Farrar, "Performance demonstration of significant availability improvement in lithography light sources using GLX control system," *Proc. SPIE 6924, Optical Microlithography XXI*, 69242Q, 2008.
- [3] E. Gross, G. G. Padmabandu, R. Ujazdowski, D. Haran and e. a. Matt Lake, "Enabling CoO improvement thru green initiatives," *Proc. SPIE 9426, Optical Microlithography XXVIII*, 942626, 2015.
- [4] V. B. Fleurov, D. J. C. III, D. J. W. Brown, P. O'Keeffe and e. a. Herve Besaucele, "Dual-chamber ultra line-narrowed excimer light source for 193-nm lithography," *Proc. SPIE 5040, Optical Microlithography XVI*, 1694, 2003.
- [5] Cymer LLC, "KrF Light Sources," [Online]. Available: <http://www.cymer.com/krf-light-sources>. [Accessed 2016].
- [6] M. T. A. T. Mike Corbett, "Semiconductor Industry Neon Capacity Disruption Continues," Linx Consulting, [Online]. Available: <http://www.semi.org/en/node/57646>. [Accessed 2016].
- [7] Gas World, "Specialty gases in 2015," *Gas World Special Feature*, pp. 34-36, February 2015.
- [8] L. Group, "Excimer Laser Gases," Linde Group, [Online]. Available: [http://www.lindeus.com/en/products\\_and\\_supply/specialty-gases/special\\_application\\_products/laser\\_gases/index.html](http://www.lindeus.com/en/products_and_supply/specialty-gases/special_application_products/laser_gases/index.html). [Accessed 2016].
- [9] J. Dorsch, "Neon Gas Supply Issues Dog the Semiconductor Industry," Semiconductor Manufacturing & Design Community, 2015.

- [10] Bourns, Inc, "Impact of Neon Gas Price Increases on Gas Discharge Tube (GDT) Devices," Riverside, California, USA, 2015.
- [11] U. K. Sengupta, "Krypton fluoride excimer laser for advanced microlithography," *Optical Engineering* 32(10), 2410—2420, 1993.
- [12] W. J. D. R. J. D. B. Kevin O'Brien, "Lithography Line Productivity Impact Using Cymer GLX™ Technology," *Optical Microlithography XXII*, Vols. 7274, 72743N, 2009.
- [13] R. J. K. O. A. R. Wayne J. Dunstan, "Increased Availability of Lithography Light Sources using Advanced Gas Management," *Optical Microlithography XX*, vol. 652032, 2007.

# **Impact of Bandwidth Variation on OPC Model Accuracy**

Will Conley, Paolo Alagna, Stephen Hsu\*, Qian Zhao\*

Cymer LLC, 17075 Thornmint Ct., San Diego, CA, 92127

\*ASML Brion, 399 West Trimble, San Jose, CA 95131

## **ABSTRACT**

Over the years, Lithography Engineers continue to focus on CD control, overlay and process capability to meet current node requirements for yield and device performance. Reducing or eliminating variability in any process will have significant impact, but the sources of variability in any lithography process are many. The goal from the light source manufacturer is to further enable capability and reduce variation through a number of parameters.<sup>(1, 2, 3, 4)</sup>

Recent improvements in bandwidth control have been realized in the XLR platform with Cymer's DynaPulse™ control technology. This reduction in bandwidth variation translates in the further reduction of CD variation in device structures<sup>5,6</sup>. The Authors will review the methodology for determining the impact that bandwidth variation has on CD dose, focus, pitch and bandwidth, which is required to build a dynamic model. This assists in understanding the impact that bandwidth variability has on the accuracy of the Source and Mask optimization and the overall OPC model, which is reviewed and demonstrated.

## **1. INTRODUCTION**

Further improvements in bandwidth variation in the XLR platform have been realized with Cymer's DynaPulse™ bandwidth control technology. This reduction in bandwidth variation could translate in to a further reduction in CD variation for device structures. The Authors will discuss the impact that these improvements in bandwidth control have on advanced lithography applications. This study investigates the impact of bandwidth on contrast sensitive device layers and these improvements will be quantified by the analysis of statistical bandwidth variation and the impact on CD.

## **2. RECENT IMPROVEMENTS IN BANDWIDTH CONTROL**

### **2.1 Experimental Conditions**

Cymer has previously discussed the capability of the DynaPulse controller demonstrating that bandwidth stability was dramatically improved over the previous generation of bandwidth controllers.<sup>5</sup> When DynaPulse is enabled on an XLR light source, the controller maintains the mean bandwidth wafer average to within  $\pm 5\text{nm}$ .<sup>6</sup> Figure 1 is a representative plot of bandwidth control over several generations of bandwidth controllers. This ranges from  $\pm 50\text{nm}$  down to a futuristic goal of  $\pm 5\text{nm}$  field to field.



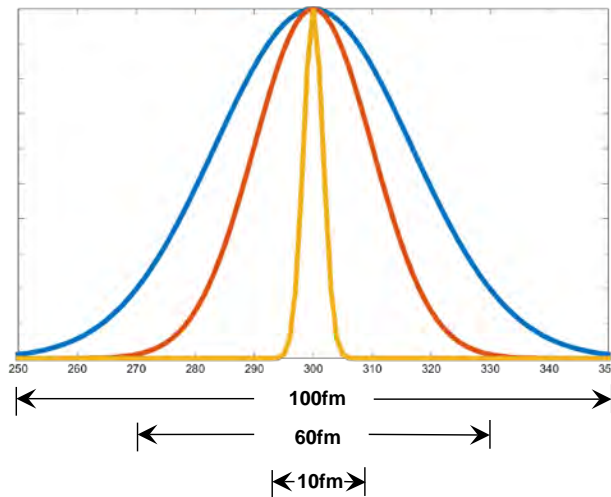


**Figure 1:** Representative plot of on wafer response to E95 modulation per field to field

### **3. PREVIOUS STUDIES “THE VARIABILITY WINDOW”**

#### **3.1 Methodology**

In previous studies have demonstrated that random bandwidth variation can contribute to random CD variation. For example, the Authors have developed a test methodology to determine the impact of bandwidth variability through the known dose and focus variability that exists in the scanner. This “variability window” demonstrates the CD variability that could exist within the test case for the baseline controller and Baseline vs. DynaPulse™ technology. This new study seeks to extend upon the prior work to determine the effect that random bandwidth variation has in the generation of data for an OPC model<sup>6</sup>.

Simulations are performed with HyperLith v7 from Panoramic Technologies. The chosen imaging conditions are 1.35NA using cQuad illumination with an outer setting of 0.87 and inner setting of 0.72. No aberrations or Jones matrix were included and the mask test site provided by Panoramic is a 90nm pitch ground rules with simple OPC applied. The mask is a standard 6% attenuated PSM calculated using Kirchoff’s approximation. An LPM positive resist model is used with a simple calibration to existing 45nm line and space imaging. The bandwidth variation for this study is 300nm (+/-50nm -baseline condition) and 300nm (+/-5nm – current condition). A focus variation of +/-14nm used, based on existing known scanner specifications.

#### **3.2 Test Site**

Figure 2 describes the 90nm pitch test site used in this study. The Authors have applied simple OPC based on the imaging and ground rules supplied by Panoramic Technologies. The calculated aerial image and imaging in positive tone photoresist are shown. In the figure below, the image at the bottom points to the three specific test locations.

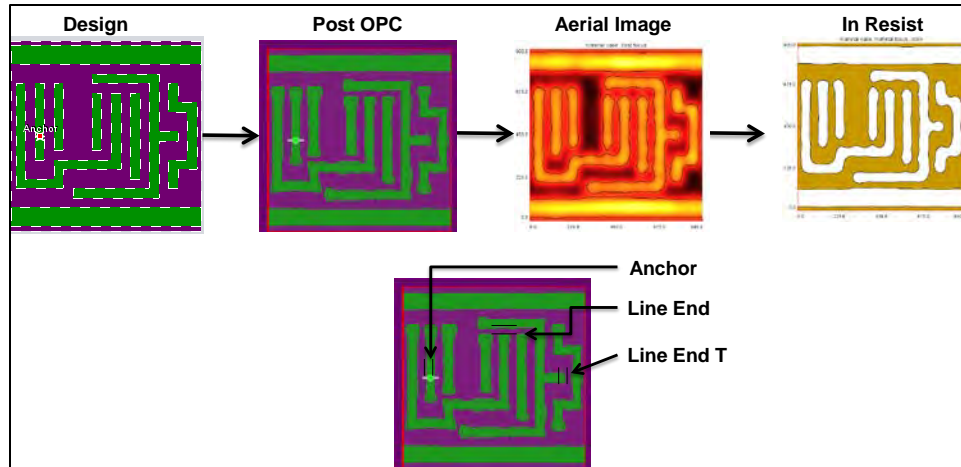


**Figure 2:** Test site for a metal layer at 90nm pitch

### 3.3 Variability Window at Best Dose through Existing Focus Variation

The Variability Window in figure 4 was determined by using the E95 bandwidth range of 300fm ( $\pm 50\text{fm}$ , baseline), dose to size only and a focus range of  $\pm 14\text{nm}$ . The amount of CD (critical dimension) variation is 1.83nm at best dose and focus.

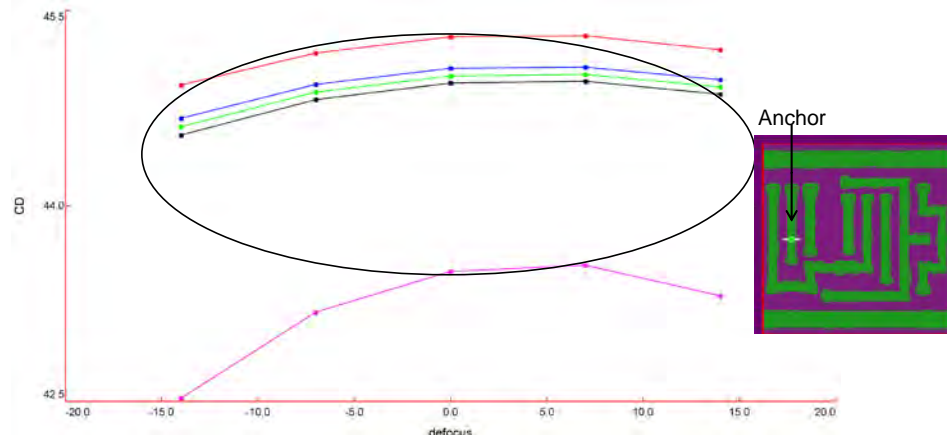


**Figure 4:** Bossung plot “Anchor” structure & “Variability Window” based on existing scanner dose / focus variation

### 3.4 Variability Window with current bandwidth control

The Variability Window shown in figure 5 was determined by using the E95 bandwidth range of 300fm ( $\pm 5\text{fm}$ , baseline), dose to size only and a focus range of  $\pm 14\text{nm}$ . The amount of CD (critical dimension) variation is 0.11nm at best dose and focus.

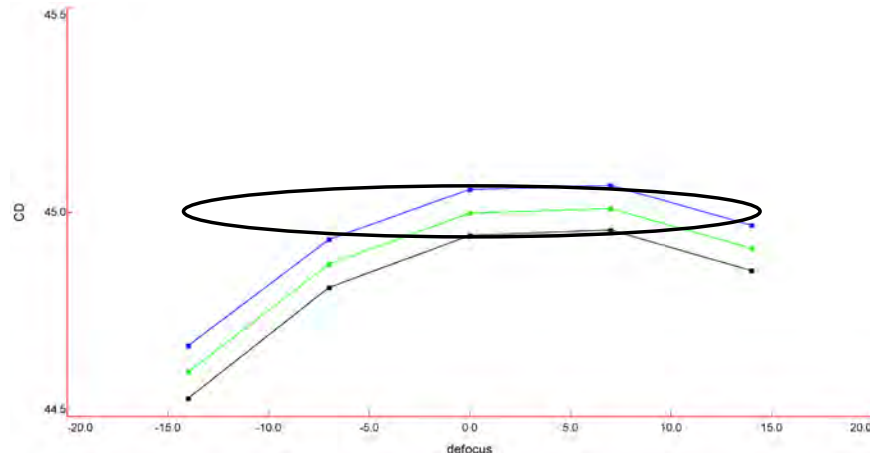


**Figure 5:** Bossung plot of “Anchor” structure & “Variability Window” single dose with current bandwidth conditions

### 3.5 Variability Window and Test Site Summary

As discussed in previous sections, the dose / focus variation conditions are  $\pm 0.45\%$  for dose and  $\pm 14\text{nm}$  for focus. The Authors would like to focus on the impact that improved bandwidth control has on CD variation from the Baseline controller to DynaPulse. The three areas of analysis from the test layout shown in section 3.2 are quantified in figure 6, the baseline at fixed dose and DynaPulse at fixed dose are plotted. The purpose is to demonstrate that dose variation as expected, has an impact on CD variation, which in these test cases, is a factor of about 2x. Additionally, plotting baseline fixed dose to DynaPulse fixed dose demonstrates even greater CD variation reduction which is about 7x-10x. However, not all structures are focus or bandwidth sensitive. In this case, the Line End structure is much more dose than focus sensitive as demonstrated in the figure 6 below. As discussed in section 3.1 the Authors have made a number of assumptions and the intention of this study is to demonstrate a methodology and a trend. From this, we see that these significant improvements in bandwidth control can affect CD variation.

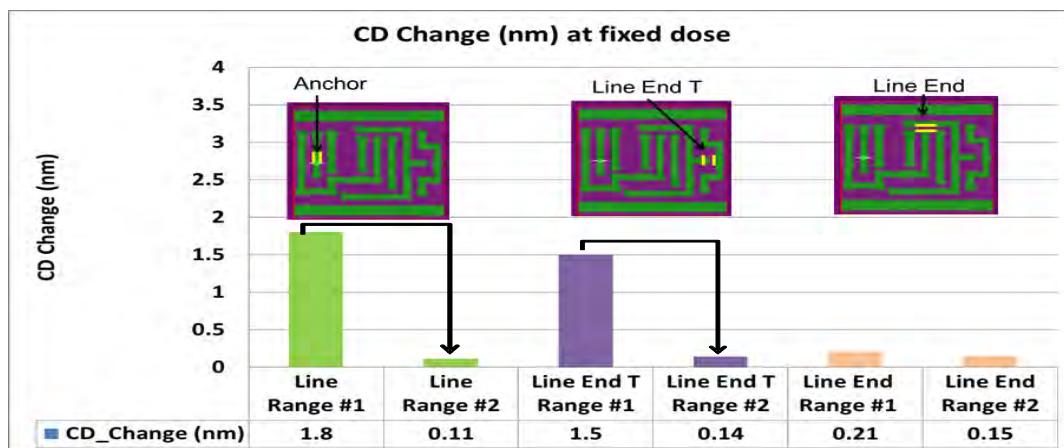
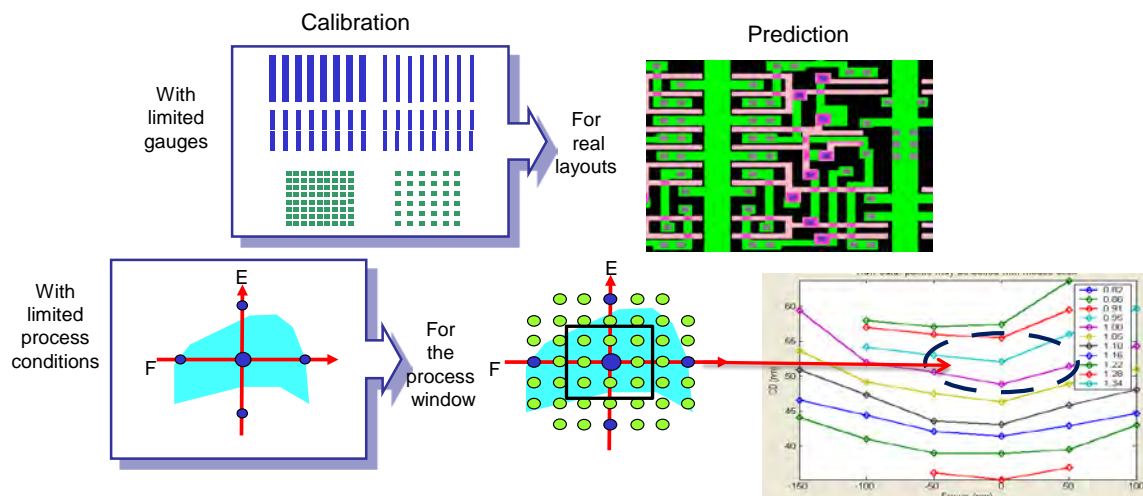


**Figure 6:** Bossung plot of “Anchor” structure & “Variability Window”

## 4. OPC GAUGE DATA CREATION

### 4.1 Test Case & Methodology with Bandwidth Variability

For this study, simulations are performed with HyperLith v7 from Panoramic Technologies. The chosen imaging conditions are 1.35NA using a custom illumination to maximize through pitch performance. No aberrations or Jones matrix were included with the mask test site provided by Panoramic being a CD target of 45nm on a pitch of 116nm to 206nm in 10nm increments with dose and focus optimized at a pitch of 126nm. The mask is a standard OMOG<sup>7</sup> mask for line and space pairs and is calculated using FDTD as provide through the Simulator. A LPM positive resist model is used with a simple calibration to existing 45nm line and space imaging. The bandwidth variation for this study is for three conditions. The first is the “legacy” controller with a center bandwidth of 300fm and a lower range of 246fm and upper range of 354fm. The second condition is the “current” controller with a center bandwidth of 300fm and a range of 270fm to 330fm and finally the third is the “future state” controller. The center bandwidth is 300fm and a range of 294-306fm. Three dose conditions of -2.5%, 0 and +2.5% along with focus conditions of +/-45nm are used.



## 5. OPC PROXIMITY CURVE THROUGH PITCH VS BANDWIDTH

### 5.1 Test Case for Bandwidth Variability

In figure 8, a plot of the CD through pitch versus bandwidth demonstrates the variation due to bandwidth in CD through pitch. The increase in CD values is shown as pitch becomes wider and this data will be used as OPC gauges to assess CD thru pitch curves at various E95 BW set point and the CD response is pre-OPC model creation with demonstration of increased CD variation through pitch vs bandwidth.



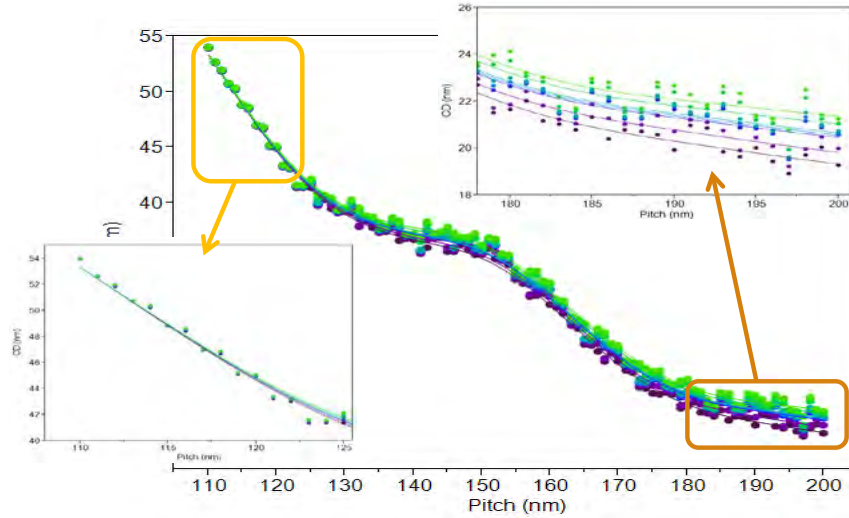


Figure 8: Proximity curve - bandwidth variation impact

## 6. BOSSUNG PLOTS THROUGH PITCH VS BANDWIDTH VARIABILITY

### 6.1 Legacy bandwidth controller through pitch

In figure 9, Bossung plots for at target CD of 45nm at three dose conditions (-2.5%, 0, +2.5%) and a focus condition of +/-45nm (15nm increments) for pitches of 126nm, 166nm and 206nm are shown. The Bossung plots are shown in the figure 9 to remind the reader of the location of in the CD through pitch plot for each of the Bossungs.

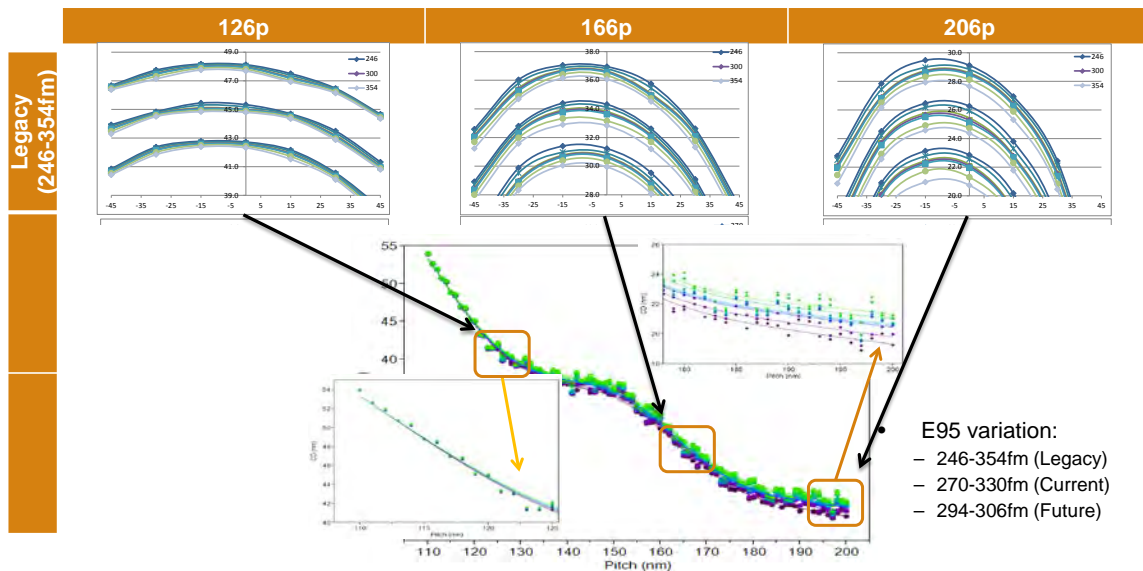


Figure 9: Bossung plots through pitch vs bandwidth (45nm initial CD Target)

### 6.2 All Bossung cases through pitch versus bandwidth

In figure 10, a matrix of Bossung plots are shown through pitch for the legacy, current and future bandwidth controllers in the y-axis and pitch in the x axis. As stated in the previous section the CD target of 45nm at threedose conditions (-2.5%, 0, +2.5%) and a focus condition of

+/-45nm (15nm increments) for pitches of 126nm, 166nm and 206nm are shown. Following each set of Bossungs down through bandwidth control, the improvement in control can be seen with less spread in each dose through focus condition. This effect becomes more evident as we investigate the through pitch effect which is mainly due to a reduction in image contrast.

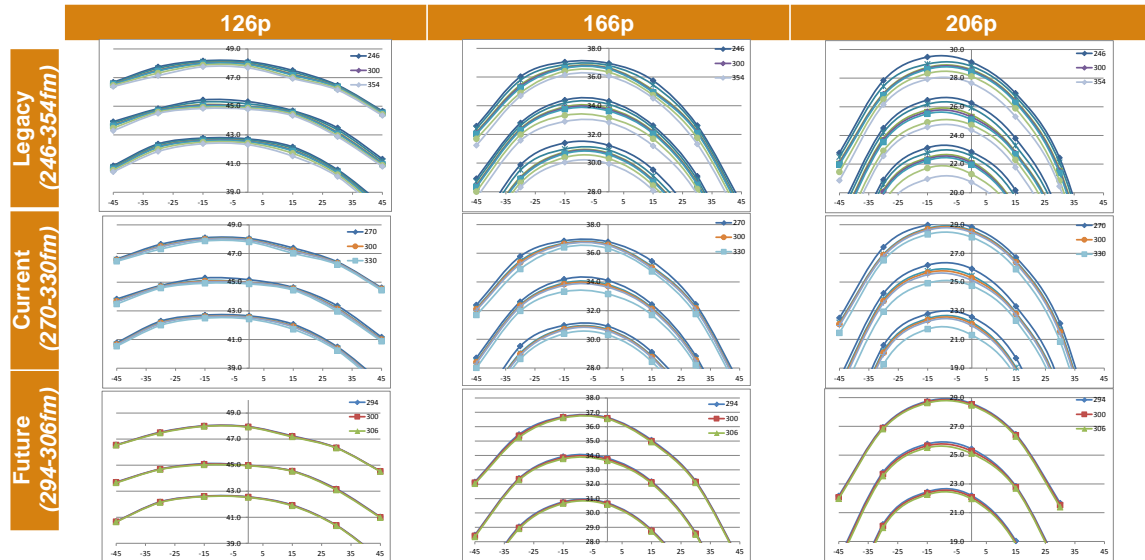


Figure 10: Bossung plot of “HotSpot” structure & “Variability Window” single dose

### 6.3 All Bossung cases through pitch versus bandwidth

In order to quantify the effect of bandwidth variation through a range of focus and dose conditions, the standard deviation is calculated for each through focus condition and bandwidth variation condition. Those calculated values are then averaged and the result is plotted below for the legacy (246-354fm), current (270-330fm) and future target (294-306fm). The response is linear with  $R^2$  demonstrating a good fit to the data. The improvement or reduction in variation from the legacy to the current controller is 1.6x greater and the current to future target is much larger at 3.8x, which demonstrates the impact that reducing bandwidth variation has through a pitch.

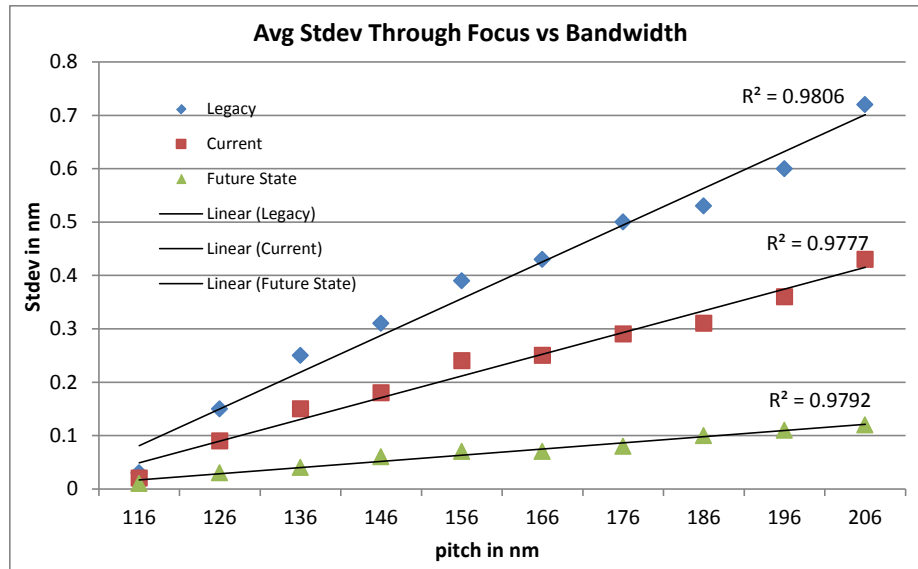
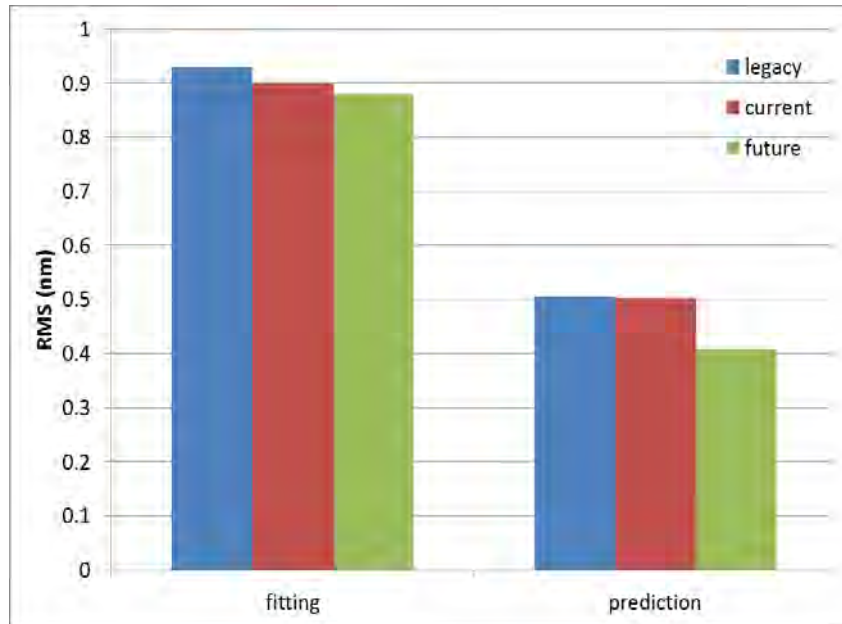


Figure 10. Stdev for each focus and dose condition averaged

## 7. DETERMINING OPC MODEL ERROR

### 7.1 Model Error

Previous work by Hunsche et al. demonstrated that OPC models could predict wafer CD variations resulting from laser BW tuning<sup>8</sup>. The focus of this work is to understand the impact that laser bandwidth variation can have on the prediction accuracy. In section, 4.1 the methodology and data generated for this study was discussed and analysis of the variation impact discussed in section 6.3. The data plotted in figure 11 is the root mean square in nanometers for the “fitting” and “prediction” of the data used for the generation of the model. The fitting is improved by nearly 10% but for prediction accuracy, this is improved by over 20% from the legacy to the future state bandwidth controller. Considering this for future nodes such as the 10, 7 or even 5nm node is significant.



**Figure 11:** Model fitting and prediction

## 5. CONCLUSIONS & FUTURE WORK

The Authors have demonstrated that bandwidth variation through pitch creates random CD variation through pitch. Bossung plots through pitch have demonstrated increased CD variation and the analysis of the data demonstrates at larger pitches nearly four times less CD variation can be achieved with improved bandwidth control. From this data and analysis, we find that OPC model predictability is improved by 20% for all pitches in the analysis. As we consider future work our focus will be to compare these models to verify impact on device layers to determine if effects translate into device layer OPC improvement with 1D and 2D structures, verify improved bandwidth control improves proximity matching (CDU improvements) and determine if this translates into device layer OPC improvement.

## 6. ACKNOWLEDGEMENTS

The Authors would like to thank Josh Thornes, Bob Socha, Greg Rechtsteiner, Emmanuel Rausa & Ronald Goossens for useful discussions, Nathan Wells for statistical guidance and the Management Teams of Brion and Cymer for their support.

## 7. REFERENCES

1. I. Lalovic et al., Defining a physically-accurate laser bandwidth input for optical proximity correction (OPC) and modeling, Proc. BACUS XXII Photomask Technology Symposium 7122 -62, (2008).
2. P. De Bisschop et al., Impact of finite laser bandwidth on the CD of L/S structures, Journal of Micro / Nanolithography, MEMS and MOEMS (JM3), Vol. 7, No. 3, (2008)
3. M. Smith et al., Modeling and Performance Metrics for Longitudinal Chromatic Aberrations, Focus-drilling, and Z-noise; Exploring excimer laser pulse-spectra," Proc. SPIE Optical Microlithography XX 6520 -127 (2007)
4. U. Iessi et al., Laser bandwidth effect on overlay budget and imaging for the 45 nm and 32nm technology nodes with immersion lithography, Proc. SPIE Optical Microlithography XXIII 7640 (2010).

5. W. Conley, et al., Improvements in Bandwidth & Wavelength Control for XLR 660ix Systems, Proc. SPIE Optical Microlithography XXVII, 90521H (2014)
6. Will Conley et al, " Impact of bandwidth on contrast sensitive structures for low k1 lithography ", Proc. SPIE 9426, Optical Microlithography XXVIII, 942607 (March 18, 2015);
7. <https://www.photomask.com/products/omog-masks>
8. Stefan Hunsche et al, "Improved Model Predictability by Machine Data in Computational Lithography and Application to Laser Bandwidth Tuning", Proc. of SPIE Vol. 7274 727405-1

# **DUV light source technologies for 10nm and below**

**Ted Cacouris, Greg Rechtsteiner, Will Conley, Paolo Alagna**

Cymer LLC, 17075 Thornmint Court, San Diego, CA 92127

## **ABSTRACT**

Deep UV light sources continue to be extended into 10nm node applications through the use of multi-patterning techniques as well as vertically integrated devices used for 3D NAND applications. The 10nm logic and DRAM devices continue to drive advanced ArF immersion patterning techniques to achieve high resolution lithography while 3D NAND devices rely more heavily on earlier-generation 248nm light sources. This paper will cover advances in light source technologies such as tighter bandwidth control to support larger focus budgets, lower bandwidth to improve image contrast and support enhanced optical proximity correction techniques<sup>1,2</sup>, as well as lower running costs. Recently, several studies exploring the impact of bandwidth on imaging performance have suggested that reducing light source bandwidth variability<sup>3</sup> can expand the focus budget as it is equivalent to reducing blur in imaging and ultimately critical dimension uniformity. Additionally, lowering the absolute bandwidth target has enabled contrast improvements that improve overall imaging margin<sup>4</sup>. Lastly, light source running costs have escalated in the past year as a result of a worldwide neon crisis where supplies were constrained and prices escalated in response. Solutions were rapidly developed to reduce consumption of neon (a key ingredient in the light source process gas) and are described here.

## **1. INTRODUCTION**

The increasing cost and complexity of lithography for advanced nodes continues to drive the need for extracting the maximum possible process yield as well as lowering running costs. The light source has contributed in making such improvements over time through tighter and more stable control and excursion avoidance, as well as by delivering efficiencies that drive lower running costs. The more recent improvements in light source performance were introduced in late 2014, including improved optical bandwidth stability which reduces wafer to wafer variability that was shown to improve CD control.

## **2. IMPROVED CD CONTROL THROUGH HIGH BANDWIDTH STABILITY**

As process margins (or process windows) continue to shrink with each advancing process node, every source of lithography variability needs to be reduced. Leveraging the experimental studies and light source technology used to create tighter wafer to wafer bandwidth stability,<sup>5</sup> further work has been pursued in simulations of tighter bandwidth control for within-wafer or field to field stability. These recent studies have shown that



additional process margin can be gained leading to improved ‘local’ CD uniformity (LCDU). The study modeled a light source with bandwidth control in the range of  $\pm 5\text{fm}$  from field to field, compared to current generation light sources that have a variation of approximately  $\pm 30\text{fm}$  (see Figure 1 below).

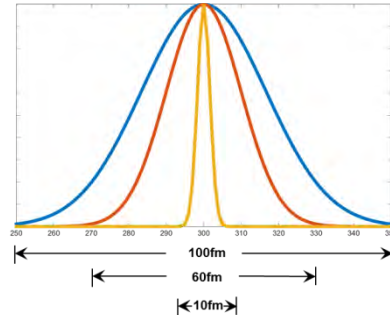


**Figure 1 - E95 bandwidth variation profiles used in this study.**

The study included a simulation of standard line-space features applicable to multiple patterning approaches with nominal feature size (CD) of 45nm. The outcome of this study has shown a progressively reduced CD variation through pitch as light source bandwidth variation is reduced. Figure 2 compares the simulated CD response of these structures through pitch using the E95 bandwidth variability shown in Figure 1.

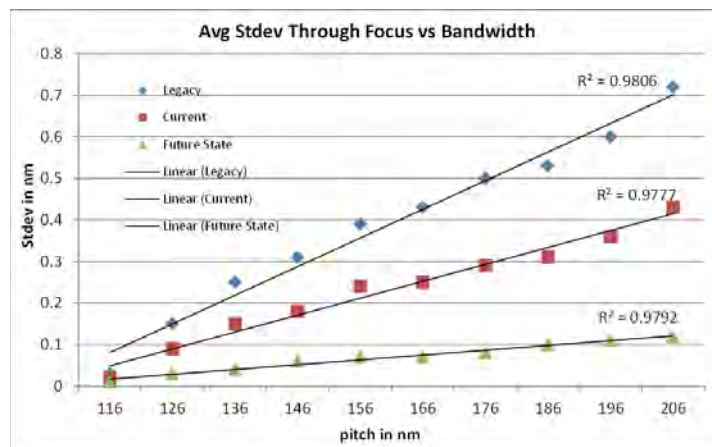


**Figure 2 - CD variation through pitch with 3 light source performance profiles.**

The results show a pronounced benefit with tighter bandwidth stability when the feature pitch is large.

### **3. IMPROVED IMAGING CONTRAST WITH LOWER LIGHT SOURCE BANDWIDTH**

In addition to improving light source bandwidth stability, further studies were pursued following initial reports<sup>6</sup> of the impact of lowering the target bandwidth. The original studies showed that there are hot spot structures in a 10nm metal 1 test structure that have an improved exposure latitude and/or depth of focus with lower nominal bandwidth targets. This triggered interest in a follow-on study where a 10nm logic device structure

was exposed under different target bandwidth settings while looking at the response of known hot spot regions. The measurements were performed after develop inspection (ADI) and some structures showed a significant response with lower bandwidth, allowing for a larger exposure latitude and even depth of focus. While not all hot spots showed a response, two examples are shown here in Figure 3, where a larger process window is observed at a lower bandwidth.

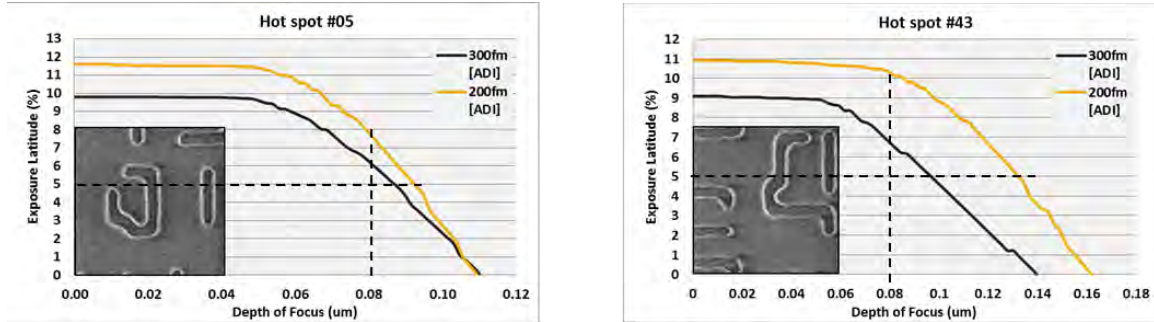


**Figure 3 - Exposure latitude and depth of focus response for nominal, 300fm bandwidth target vs. lower, 200fm bandwidth.**

As an extension to this concept, there is an opportunity to use bandwidth as an input variable in the creation of OPC models, which can offer additional exposure latitude or improved imaging characteristics at more aggressive nodes<sup>7</sup>. Initial work in this area suggests that semi-isolated structures, such as cut masks can benefit with higher exposure latitude and depth of focus; experimental work is planned to generate masks optimized at nominal and low bandwidth targets in order to measure on-wafer impact directly.

#### **4. TUNABLE BANDWIDTH LIGHT SOURCE TECHNOLOGY**

The encouraging results from these studies are driving the development of new light source capabilities, both in addressing lower bandwidth as well as improved stability. To achieve a nominally lower E95 light source bandwidth, there are at least two key components in the light source that require change: the line narrowing module (LNM) which forms one of the wavelength-selective reflectors in the excimer laser cavity, and the bandwidth metrology (BAM) that measures real-time bandwidth performance to support a closed-loop control architecture. The LNM is comprised of a grating element that acts as a wavelength-selective reflector, and includes optical prisms to adjust the angle of incidence and dispersion of light onto the grating, thus controlling both wavelength and bandwidth (see Figure 4). Given that the application of low bandwidth technology may not be broadly applied to all lithography layers in a multi-patterning scheme, the light source control system needs to drive to a target bandwidth commanded from the lithography tool based on the recipe needed to expose a layer. This would provide flexibility in selecting optimal targets based on masks that can benefit from lower bandwidth exposure vs. those that will need the standard, 300fm target. The requirement to realize this recipe-selectable bandwidth change is the need to switch and stabilize to a new value within 8 seconds, the time it takes for the next wafer lot to start. Feasibility studies have demonstrated this hardware and software capability to be achievable, as shown in Figure 5.

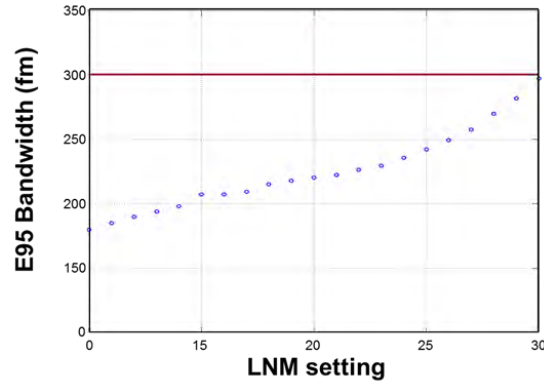


**Figure 4 - Proof of concept design showing the ability to select a target E95 bandwidth via LNM controls.**

Initial system studies also show the potential of having a counteracting attribute with lower bandwidth, namely the expected increase in speckle, or spatial coherence. This could reduce the potential benefit of lower bandwidth by increasing the linewidth roughness (LWR) of features that could be measured as an increase in CDU. While these studies highlight this theoretical effect, initial on-wafer studies have not shown any noticeable LWR with lower bandwidth. Additional characterization studies will be needed to fully understand the impact of speckle vs. improved image contrast.

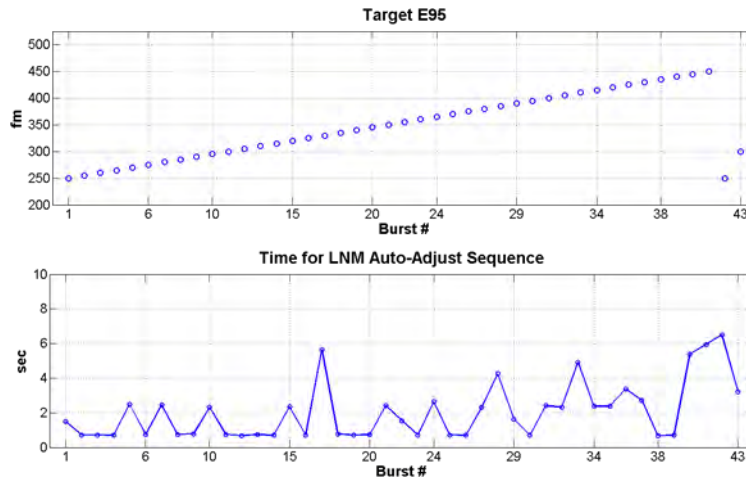


**Figure 5 - E95 bandwidth switching speed (lower chart) as the LNM is commanded to step up at 5fm increments from 250fm and back down (upper chart).**

## 5. REDUCING OPERATING COSTS FOR LITHOGRAPHY

One of the key contributors to lithography running costs is the light source, and one of the main materials that is consumed by the light source is the chamber gas. In both ArF and KrF (193 and 248nm, respectively) light sources, the gases used in the excimer discharge chambers contain neon as the buffer gas (~96%) in a mixture that includes argon, fluorine and xenon for ArF light sources, and krypton, fluorine and xenon in the KrF light sources. To maintain stable operation over time, the gas in the discharge chambers is replenished and replaced periodically to prevent a buildup of by-products and contaminants from the discharge. Early in 2015, the cost of neon spiked up

dramatically, increasing tenfold or higher due to a supply chain disruption<sup>8</sup>. The increase in neon pricing overshadowed all other lithography running costs and furthermore, there were indications of a supply constraint that could lead to fabs shutting down. The semiconductor industry is the leading consumer (~70%) of all worldwide neon production, primarily due to the DUV light sources for photolithography.

In response to this neon crisis, several parallel efforts were taken to reduce consumption as well as design longer-term solutions that would include recycling of spent neon gas. To reduce neon consumption, the gas control algorithms were re-optimized and new, fail-safe features introduced to allow consumption to be ultimately reduced by a factor of 4. This work was done in two steps: first, a factor of two reduction in consumption was achieved with gas control changes in the light source, followed by another factor of two several months later. Close performance monitoring and a very large scale testing protocol involving close collaboration with the users (fabs) led to rapid confidence building of the solutions (Figure 6). This rapid development dramatically reduced neon demand which had the desired effect of driving pricing down and loosening the supply chain constraints.

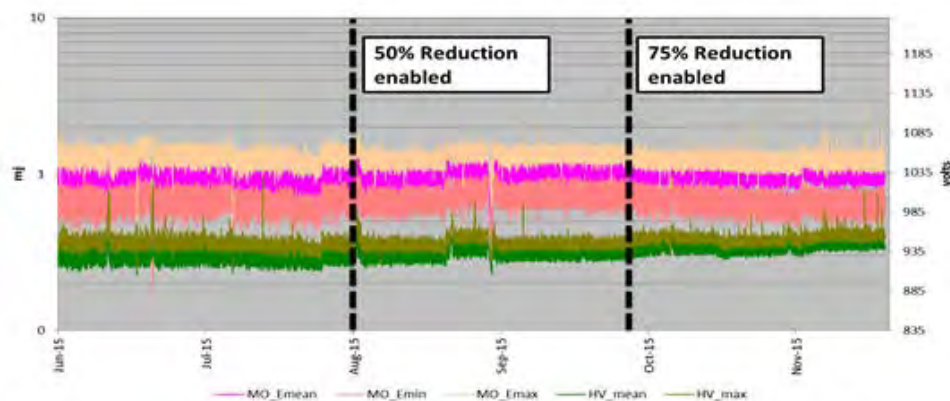


**Figure 6 - Key excimer light source system parameters indicating stable operation as the system transitioned across 2 levels of neon reduction.**

A very extensive field trial was performed across multiple fabs and tools to gather sufficient data in a short period and confirm performance stability of these solutions. Results from this field trial are shown in Figure 7, where gas consumption is measured in terms of usage in liters per billion pulses (laser firing). Since gas control algorithms dynamically adjust the rate of addition (injects) and refresh (refill) based on use conditions (utilization), the consumption rate will vary somewhat as is reflected in the chart. Beyond these changes, a local gas recycling system is under development that will further reduce the need for neon by capturing the effluent and re-purifying it at a fab level.

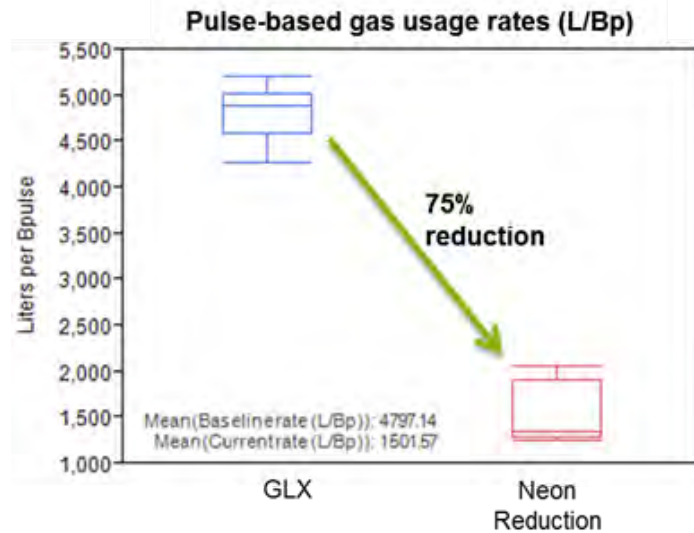


**Figure 7 - Results from the neon reduction field trials showing gas consumption in liters per billion pulses.**

## 6. SUMMARY

New light source technologies continue to be developed for DUV lithography as these tools are extended to 10nm and below, addressing process improvements through broadening of process windows or increased margins, as well as creating new opportunities for further optimization or refinement. The ability to reduce bandwidth variability to effectively eliminate bandwidth as a contributor to CD uniformity as well as lower the nominal bandwidth operating point to further optimize OPC designs offer paths to continue to extend DUV at 10nm and below. Additionally, an unexpected increase in light source operating cost resulting from a neon crisis was rapidly redressed by novel gas control modifications and implemented successfully through close collaboration with fab users.

## References

- <sup>1</sup> R.C. Peng et al. "Effects of laser bandwidth on Iso-Dense Bias and Line End Shortening at sub-micron process node" Proc. SPIE 2007, Optical Microlithography XX - Vol. 6520
- <sup>2</sup> U. Iessi et al. "Laser bandwidth effect on overlay budget and imaging for the 45 nm and 32nm technology nodes with immersion lithography", Proc. SPIE 2010, Optical Microlithography XXIII, 76402.
- <sup>3</sup> W. Conley et al., "Impact of bandwidth on constant sensitive structures for low k1 lithography" Proc. SPIE 2015, Optical Microlithography XXVIII, 942607
- <sup>4</sup> P. Alagna et al., "Optimum ArFi laser bandwidth for 10nm node logic imaging performance" Proc. SPIE 2015, Optical Microlithography XXVIII, 942609.
- <sup>5</sup> T. Cacouris et al., "New ArF immersion light source introduces technologies for high-volume 14nm manufacturing and beyond", SPIE Microlithography Symposium 2015, Optical Microlithography XXVIII.

---

<sup>6</sup> P. Alagna et al., “Advanced Process Characterization using Light Source Performance Modulation and Monitoring”, SPIE Microlithography Symposium 2015, Optical Microlithography XXVIII.

<sup>7</sup> P. Alagna et al., “Lower bandwidth and its impact on the patterning performance”, SPIE Microlithography Symposium 2016, Optical Microlithography XXIX.

<sup>8</sup> T. Cacouris, Emmanuel Rausa, “How one light source manufacturer overcame the 2015 neon crisis”, Photonics Online, November 12, 2015, [www.photonicsonline.com](http://www.photonicsonline.com).



# Means to improve light source productivity: from proof of concept to field implementation

E. Rausa, T. Cacouris, W. Conley, M. Jackson, S. Luo, S. Murthy, G. Rechtsteiner, K. Steiner  
Cymer LLC (an ASML Company),  
17075 Thornmint Ct., San Diego, CA, 92127, USA

## Introduction

Light source technological performance is key to enabling chipmaker yield and production success. Just as important is ensuring that performance is consistent over time to help maintain as high an uptime as possible on litho-cells (scanner and track combination). While it is common to see average tool uptime of over 99% based on service intervention time, we will show that there are opportunities to improve equipment availability through a multifaceted approach that can deliver favorable results and significantly improve on the actual production efficiency of equipment.

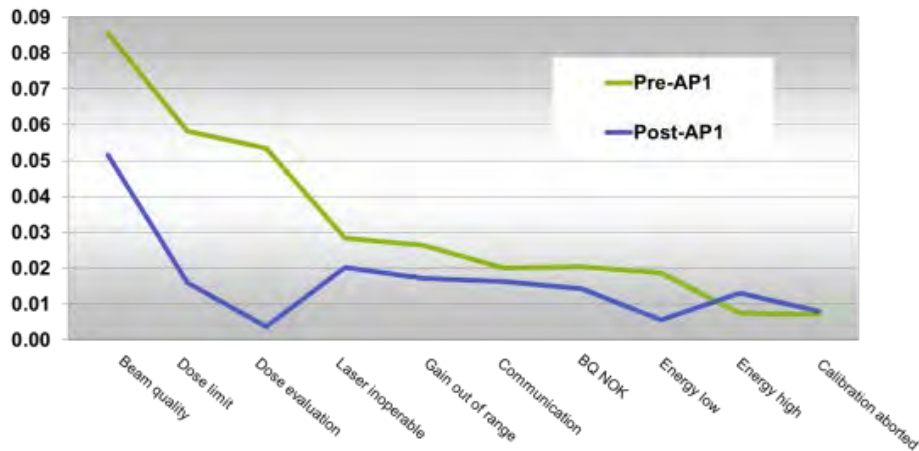
The majority of chipmakers are putting light source data generated by tools such as Cymer OnLine (COL), OnPulse Plus, and SmartPulse to good use. These data sets, combined with in-depth knowledge of the equipment, makes it possible to draw powerful conclusions that help increase both chip manufacturing consistency as well as equipment productivity. This discussion will focus on the latter, equipment availability, and how data analysis can help increase equipment availability for Cymer customers.

There are several types of opportunities for increasing equipment availability, but in general we can focus on two primary categories: 1) scheduled downtime and 2) unscheduled downtime. For equipment that is under control of a larger entity, as the laser is to the scanner, there are additional categories related to either communication errors or better synchronization of events that can maximize overall litho-cell efficiency. In this article we will focus on general availability without highlighting the specific cause of litho-cell (laser, scanner and track). The goal is to increase equipment available time with a primary focus is on opportunities to minimize errors and variabilities.

## AP1 development and implementation.

Cymer has a systematic, long-term effort on proactive reduction errors as part of our commitment to continuous improvement. Analysis of light source data has identified ten large event contributors. These events were related to the light source beam properties such as dose, dose control, gain, and beam quality. The Pareto distribution shows that these elements are responsible for over 80% of the errors or warnings generated; therefore, a solution expected to reduce many of these errors was designed. An illustration of the specific errors and their rate before and after AP1 is presented in graph 1.

## Graph 1: Error rate Pareto comparison (sample size>200)

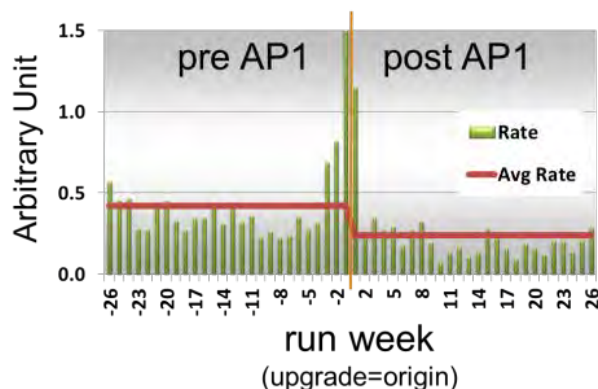


The AP1 solution was implemented, and detailed monitoring of field performance was performed. A 40% overall error reduction was achieved. It should be noted that this paper is only reporting on the error rate Pareto chart. A related yet different study can be performed looking not only at the frequency of error generation as done here, but by looking at the impact of errors on litho-cell availability. The distribution would naturally lead to a different Pareto and different strategy to be implemented. At Cymer our goal is to reduce both error generation frequency as well as the production time loss associated with errors. Please note that some of the errors listed here do not interrupt production; they are simple warnings but are included as customers monitor both warnings and errors.

Overall we can estimate an error rate reduction *that* contributed 25 hours of increased uptime on the litho- cell.

It is interesting to note that the AP1 implementation quickly demonstrated that the error rate reduction was not, as expected, constant over time. Instead, as shown in graph 2, the error rate for the first week after implementation was higher than for any other week after that over the next six months.

Graph 2: Error rate vs chamber life(sample >200)



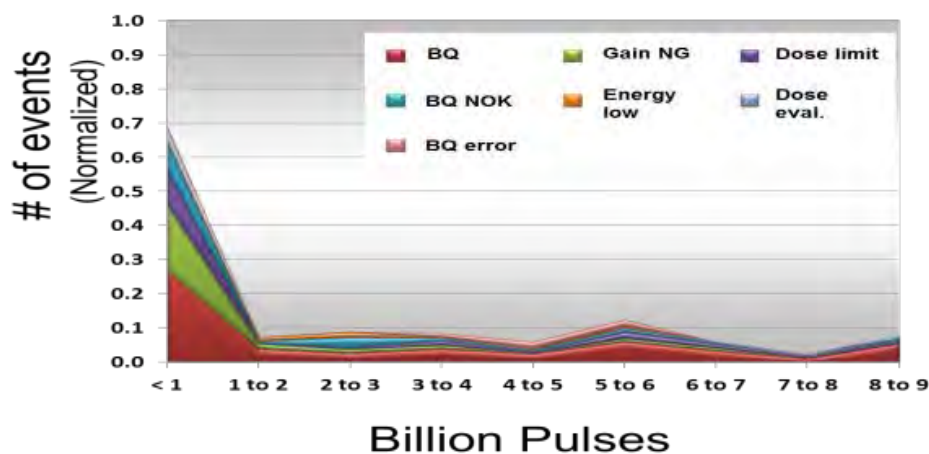
Analysis of more than 200 implementations found that this signature was not related to the install of the solution itself. But rather, the spike in error rate was found to be periodic in nature and correlated to the chamber life. The

correlation with the install time was caused by the implementation timing: in order to minimize overall equipment downtime the AP1 upgrade was aligned with a scheduled preventive maintenance event that consisted, in most cases, of a chamber replacement. This was later verified by observing repetition of this higher error rate during the first week after changing the Master Oscillator (MO) and Power Amplifier (PA) chambers.

Further improvement with AP2

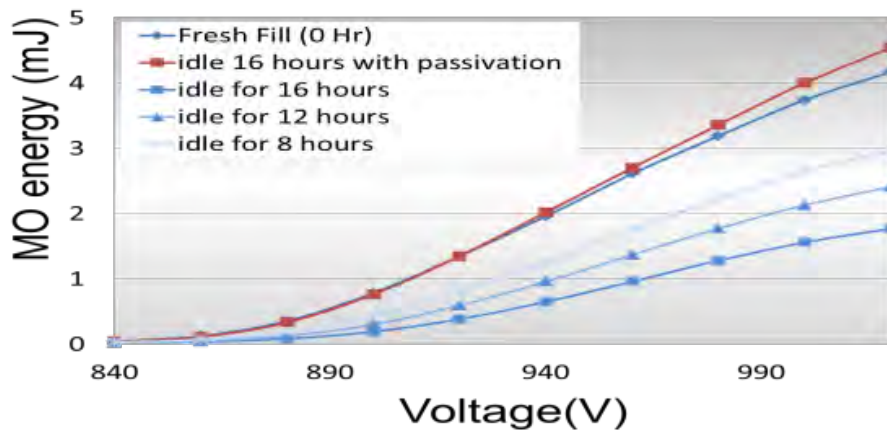
A closer study of this week after a service event showed a specific Pareto trace (graph 3) linked to that period of time. It can be seen that the error was generated because the laser was not delivering the expected power.

### Graph 3: Top seven error contribution



The error rate spike is dependent not only on time and chamber age (in Billion Pulses), but also on laser use pattern and idle time. This traces back to a variation in the MO chamber energy efficiency as a function of laser idle time in early life. Graph 4 shows results of an experiment conducted by Cymer showing MO energy variation as a function of laser idle time. With previous configurations, the MO chamber efficiency would lower almost linearly as a function of idle time. The MO efficiency would decrease more than half in a period of 16 hours idle time. With the introduction of a Cymer passivation solution, the MO chamber energy efficiency is maintained over long idle periods. This is one example of data analysis highlighting an issue with the fundamental design and assisting in the development of a solution targeted at such a specific issue.

### Graph 4: Idle time effect on efficiency

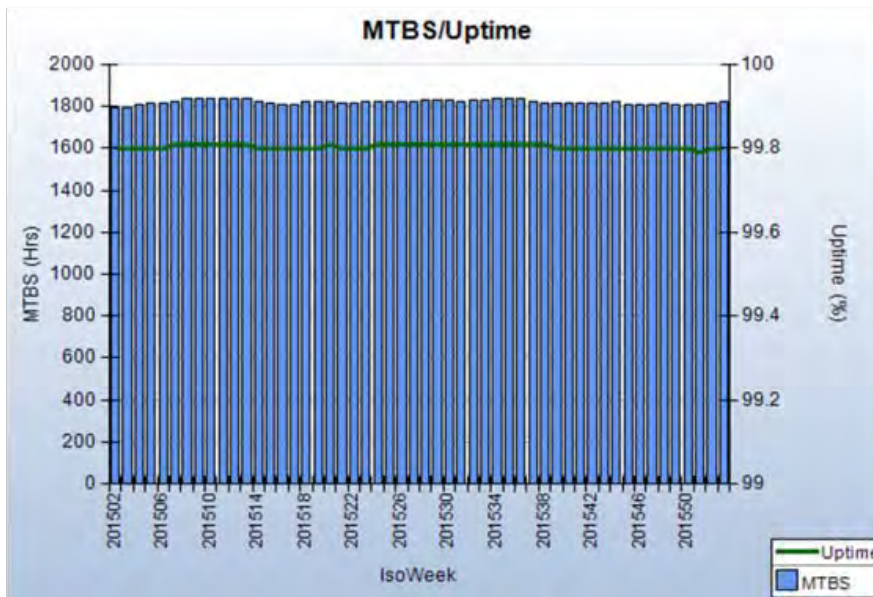


Focusing on this particular behavior lead to a better insight into the physics and chemistry of the design and, subsequently, a more robust solution. The solution introduced was confirmed to deliver fewer errors and refills in the chamber early life stages. and significant Neon savings in the long-term is expected. The error reduction and other time savings measures in AP2 are expected to deliver significant improvement in litho-cell uptime comparable to AP1 savings. This will be verified by means of implementation monitoring, using a methodology similar to that used for the AP1 release.

#### Light source availability

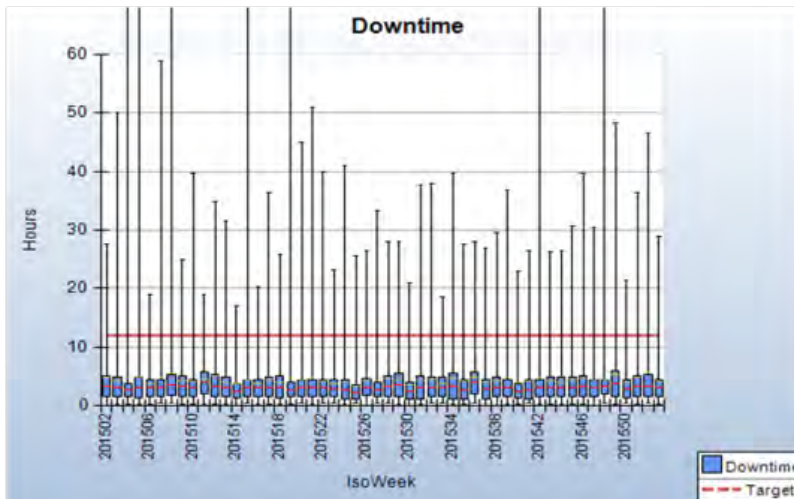
Graph 5 was created by compiling service reports that monitor the amount of time Cymer services the equipment, either performing scheduled preventive maintenance activities or unscheduled maintenance activities. The graph shows that, over the extensive install base of equipment under a service contract, Cymer light sources have a very stable average MTBS of 1800 hours and overall equipment uptime well above 99%. This comparatively high uptime is uncommon amongst semiconductor manufacturing equipment. It is one that is however necessary to maintain and improve as the laser is required for scanner operation and therefore directly impacts the scanner and litho-cell total uptime.

#### Graph 5: Uptime over 1 year



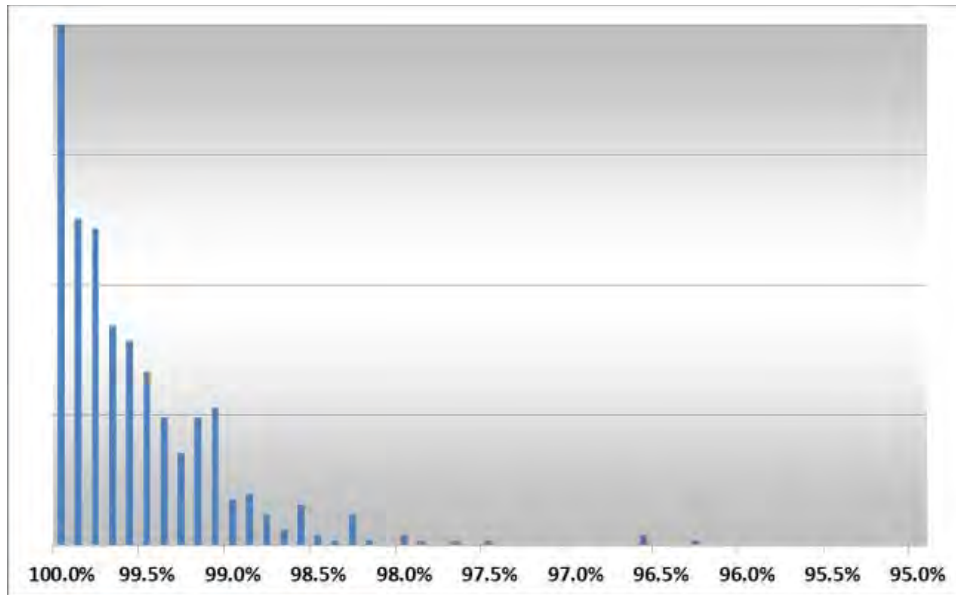
Equipment uptime and its corollary, equipment downtime, is very stable on average. A light source downtime average is approximately three hours across the entire install base, yet one can see on Graph 6 that the deviation from average downtime over an extended period is high. In fact, maximum downtime can be many times that of the mean downtime itself.

Graph 6: Downtime variation over 1 year



We should highlight that the seemingly large variation in downtime on Graph 6 is not in contradiction with the uptime stability of Graph 5. The difference is statistical; the set of data plotted on Graph 6 is a subset of the sample set used in Graph 5. One set is the whole population, the other consist of only the tools that experienced a downtime event. Graph 7 illustrates this and puts in perspective the large number of tools with little or no downtime.

Graph 7: Tool uptime distribution over a 13-week period



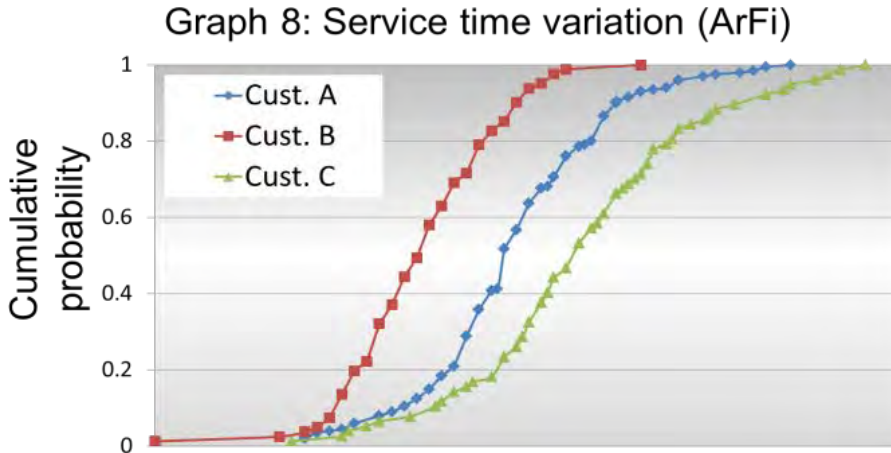
A second explanation for the variation in downtime is found by looking at what constitutes downtime. Downtime has two very different aspects to it: 1) regularly scheduled, well-defined preventive maintenance, and 2) unscheduled maintenance. That unscheduled time is characterized by an unexpected failure. Repair time in those instances varies due to the steps required to arrive at a resolution: analyze symptoms, identify primary root cause and related failures, replace/repair, validate solution, and verify performance. Scheduled events have fewer steps because the system status is good to start with and therefore the source of variations ought to be smaller.

For Cymer and its customers the focus is on down events as they are causing critical production stoppage. To minimize Cymer light source downtime we look at means to reduce equipment failures by ongoing improvement projects that involve hardware and software design changes. This is the more classical approach of a Continuous Improvement Program (CIP).

#### Impact of service on equipment downtime variation

We can also impact the overall downtime by understanding the variability of downtime that is not equipment-related. Using the same data sets, we can see service time variation (Graph 8).





Customer B service events are shorter with less time variation than those of Customer C. Another way to look at the data is that the average service time at Customer B is only achieved ~10% of time at Customers A and C. These are large differences that can and should be minimized though training as well as systematic approaches and controls.

The methodology and approach to service can also affect the balance of scheduled versus unscheduled events as well as the service time repeatability of both scheduled and unscheduled events. In a controlled experiment performed with a customer, service events over a statistically significant period of time to produce valid results were recorded. The results of this project are illustrated in Table 1 and are compared with rest of the world wide data in order to provide more context. One can see that the case study consisting of a different service scheme for scheduled events and that scheme leads to a significant reduction in unscheduled downtime.

		Case study		Rest of the World	
		downtime	stdev (a.u.)	downtime	stdev (a.u.)
ArFd	Scheduled	84%	54	69%	64
	Unscheduled	16%	31	31%	100
ArFi	Scheduled	83%	53	77%	93
	Unscheduled	17%	44	23%	100

**Table 1 : Service model impact on Unscheduled downtime and variation in MTTR**

The ratio of scheduled versus unscheduled downtime for equipment in this case study is consistent across platforms at about 17% of total downtime. For the rest of the world, i.e. customers under various service plans, the unscheduled downtime could represent as much as 30% of the total downtime. This is a 50% improvement in unscheduled downtime for that tool set. It is also important to note that the standard deviation around a service time event, for both scheduled and unscheduled events, also improved. These results are significant because the impact of an unscheduled event is far more severe on fab output than that of a planned event.

Total litho-cell downtime related to light source downtime is in fact longer than the light source downtime due to the need for various recalibrations and tests required to ensure the wafer production is within process specifications. Additionally, unscheduled events on litho-cells proved even more difficult to manage in recent years. This is due to the complexity and difficulty of maintaining low overlay while using multi-patterning to generate features much smaller than the light source wavelength. Many critical layers are now running on dedicated scanner and chuck overlay strategies. The technique is efficient and widely used. .

As a result, an unplanned interruption of litho-cell manufacturing may impact not only a single lot and its rework; it is likely to reduce or stop completion of several critical production steps of lot run before the errors, too. They must be queued up to wait for a particular litho-cell to restart, significantly increasing the lot average cycle time.

## Conclusion

Opportunities to improve light source availability can be identified through systematic review of data. There are several different approaches that can be used to identify potential improvements. Errors and interrupts can be addressed by software solutions through communication protocol enhancement or with a better understanding of the underlying design and physical characteristics. General application of CIPs will address some potential improvements. Human know-how, training, and standardization of processes also have potential for improving downtime variability and, therefore, increase predictability of litho-cell return to production states.

